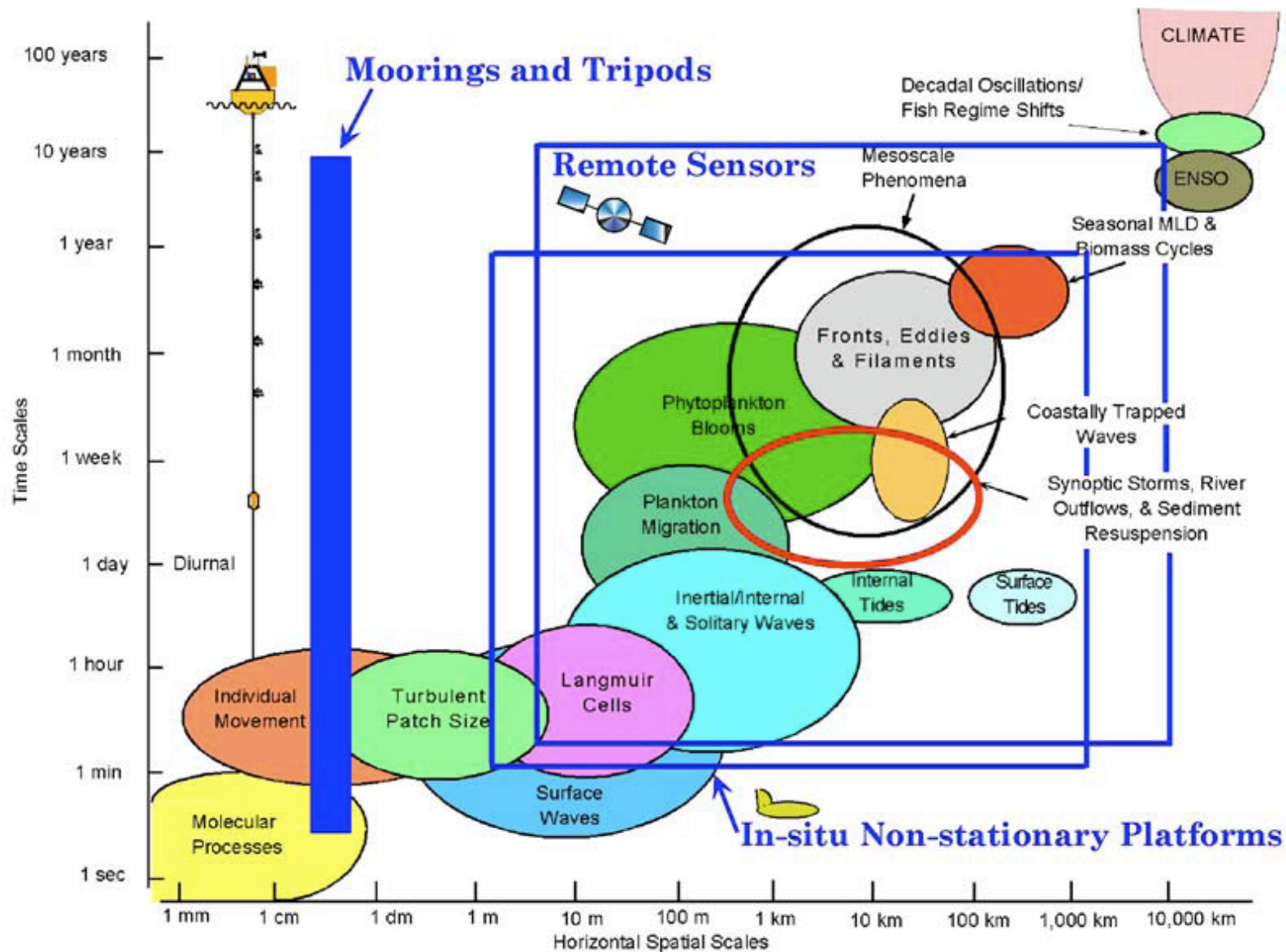


# Oceanic Measurements and Large-Scale Patterns



The range of space and time scales for a variety of ocean phenomena, and the types of observational platforms from which they can be measured (Dickey, 2001). Climate here includes the large-scale circulation. Both moving platforms (floats) and remote sensors (satellites) are extending their sampling further to the upper-right. Ice and sediment cores reach even longer times.

# Ship-Based Observations



## Pros/Cons:

Only option for many measurements  
Ability to do process studies  
Only way to get full depth information  
Expensive and difficult

## Key Results:

Bathymetry  
Surface properties (T, S, nutrients)  
MLD/Stratification  
Water mass distributions  
Deep water circulation (C14)  
Sediments (paleoclimate)

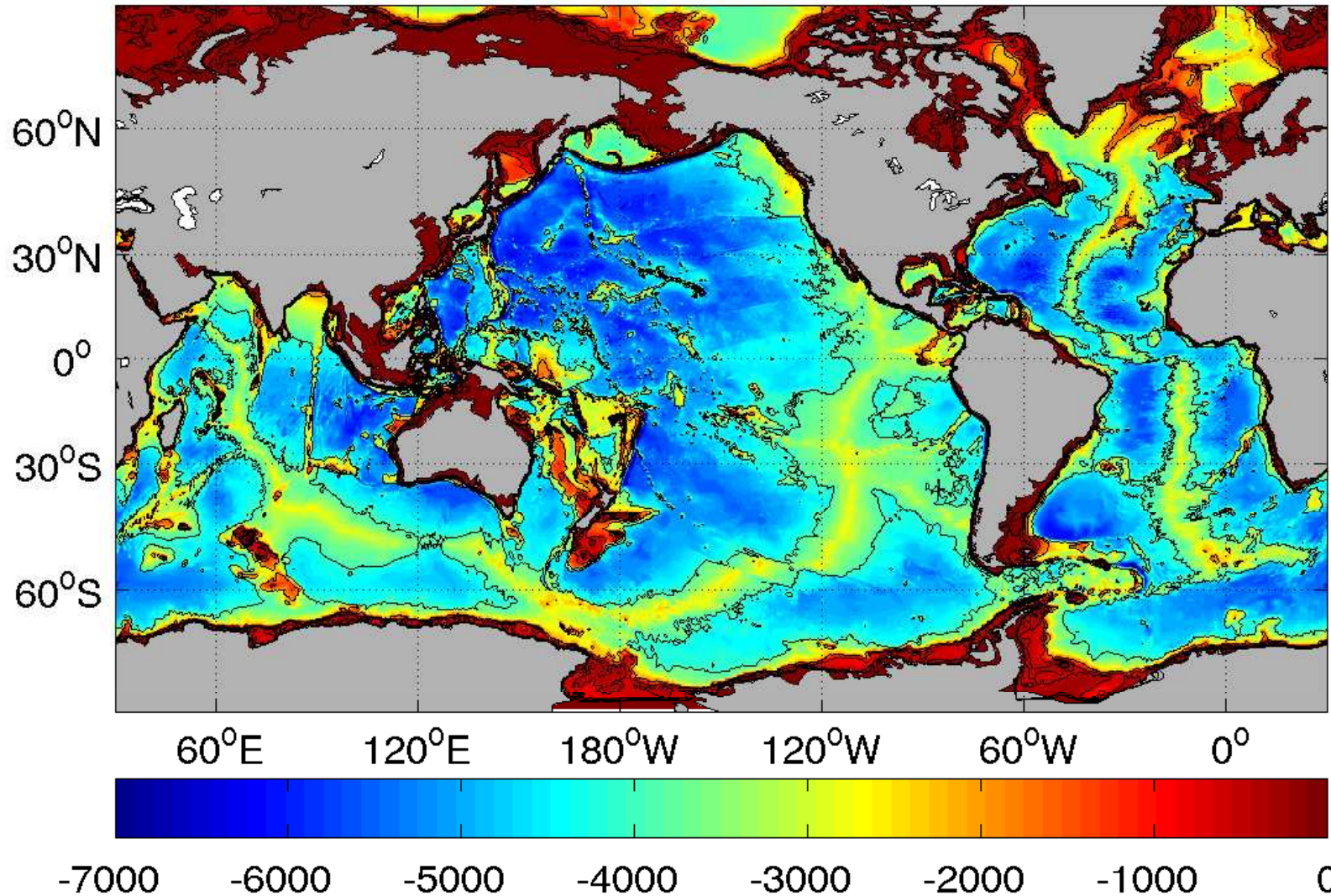
**Concept:** Ships are remarkably inefficient sampling platforms: limited duration, slow speed, narrow field of view, and often uncomfortable if not dangerous.

Only well-instrumented ships on many cruises over many years have begun to cover the world's oceans. While ship instrumentation has improved greatly over recent decades, ship sampling efficiency has not. Remote sensing and autonomous instrumented platforms can do very much better, and they offer a better present and future for oceanic measurements.

The ocean is highly undersampled compared to the variability of its currents and dissolved and particulate material concentrations. It still is a scientific frontier.



# Bathymetry



Oceanic bottom depth [m] measured by acoustic sounding, *i.e.*, from the time it takes for short bursts of 20Hz sound to echo back to the ship. This method has the best accuracy (about 1%), and has been routinely done on nearly all ships. Bathymetry influences ocean circulation, differentiates biological habitat, and creates extreme environments, *e.g.*, hydrothermal vents.

Notice the continental shelves, mid-ocean ridges, and narrow trenches.



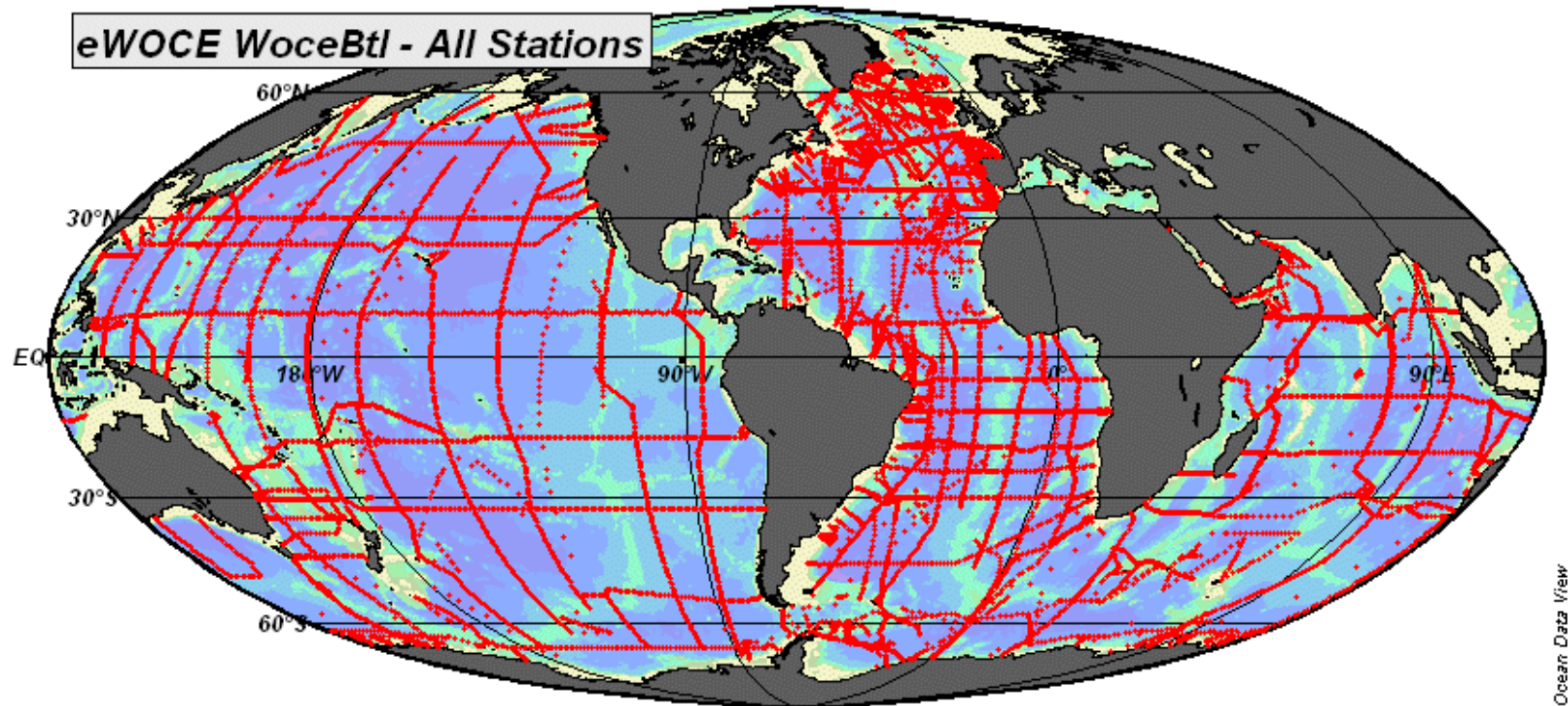
**Concept:** Oceanic basins are produced by plate tectonics.

Without a geophysically active interior for the Earth, the planet would be an “aqua world” and we would have gills.

Conspicuous bathymetric features are mid-ocean ridges (plate spreading centers) and deep trenches (plate subduction zones). Secondary influences are sedimentation from land erosion and rivers and shoreline erosion from surface waves.

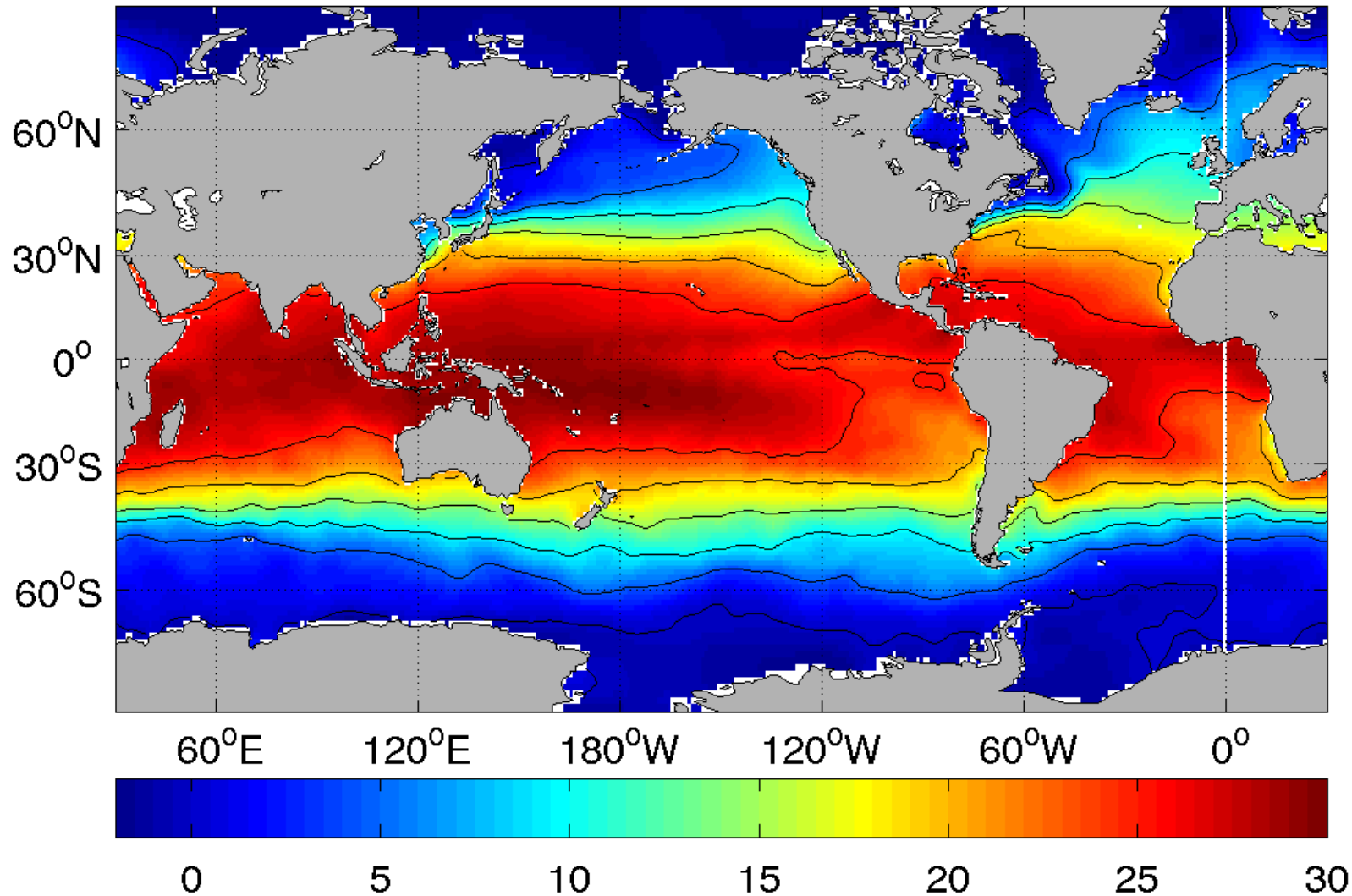
Millions and billions of years ago, the basins were very differently shaped.

# Hydrographic Surveys



The World Ocean Circulation Experiment in the 1990s was the first systematic global survey of the ocean for a large number of physical, chemical, and biological (material) properties measured from ships. WOCE “sections” and their repeats (CLIVAR) led to modern climatologies of oceanic water masses, *e.g.*, the World Ocean Atlas [<http://www.ewoce.org>]. In most places ship measurements do not include direct current measurements relevant to long-time averages (years) because short-term fluctuations are large.

# Sea Surface Temperature



Annual mean temperature  $T$  [ $^{\circ}\text{C}$ ] at the surface (SST) (World Ocean Atlas, 2005). Oceanic temperature is now typically measured with a thermistor on a CTD that simultaneously measures electrical conductivity (C), temperature (T), and pressure (hydrostatically converted to depth, D). SST also is measured by radiometry from satellites. Notice warm tropics, cold poles. Deviations from the zonal mean reflect the influence of large-scale horizontal circulation.

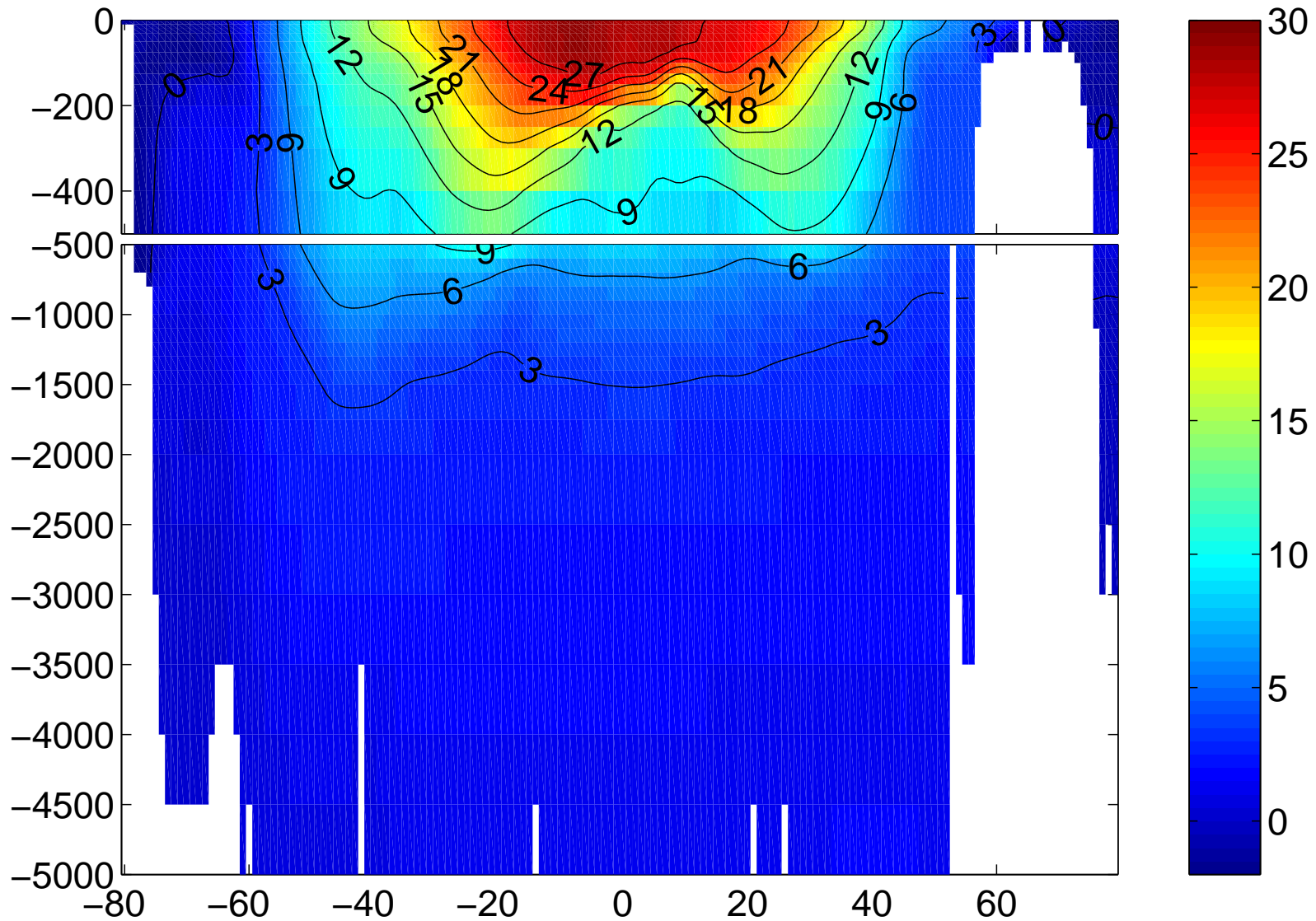


**Concept:** The two most immediate effects of the ocean on the atmosphere are the drag it provides on surface wind (mostly through generating surface waves) and the thermal reservoir it presents through its SST.

These immediate effects matter on time scales of hours or less.

On longer time scales, SST is influenced by the entire ocean, and the ocean is a major component of Earth's climate and climate variability.

# Temperature Section (Pacific)



Annual mean  $T$ (latitude [ $^{\circ}$ N], depth [m]) [C] along 170W in the Pacific (World Ocean Atlas, 2005). Warm water is lighter and “floats”. The density stratification  $\rho(z)$  is primarily due to  $T(z)$ , with important exceptions in polar regions, where salinity  $S$  is key because thermal expansion is small (also near rivers). The “warm-water sphere” is bounded by the thermocline, usually also the pycnocline in  $\rho(z)$ .

**Concept:** The ocean is stably stratified in density, with

$$\rho \approx \rho_0(1 - \alpha(T - T_0) + \beta(S - S_0)),$$

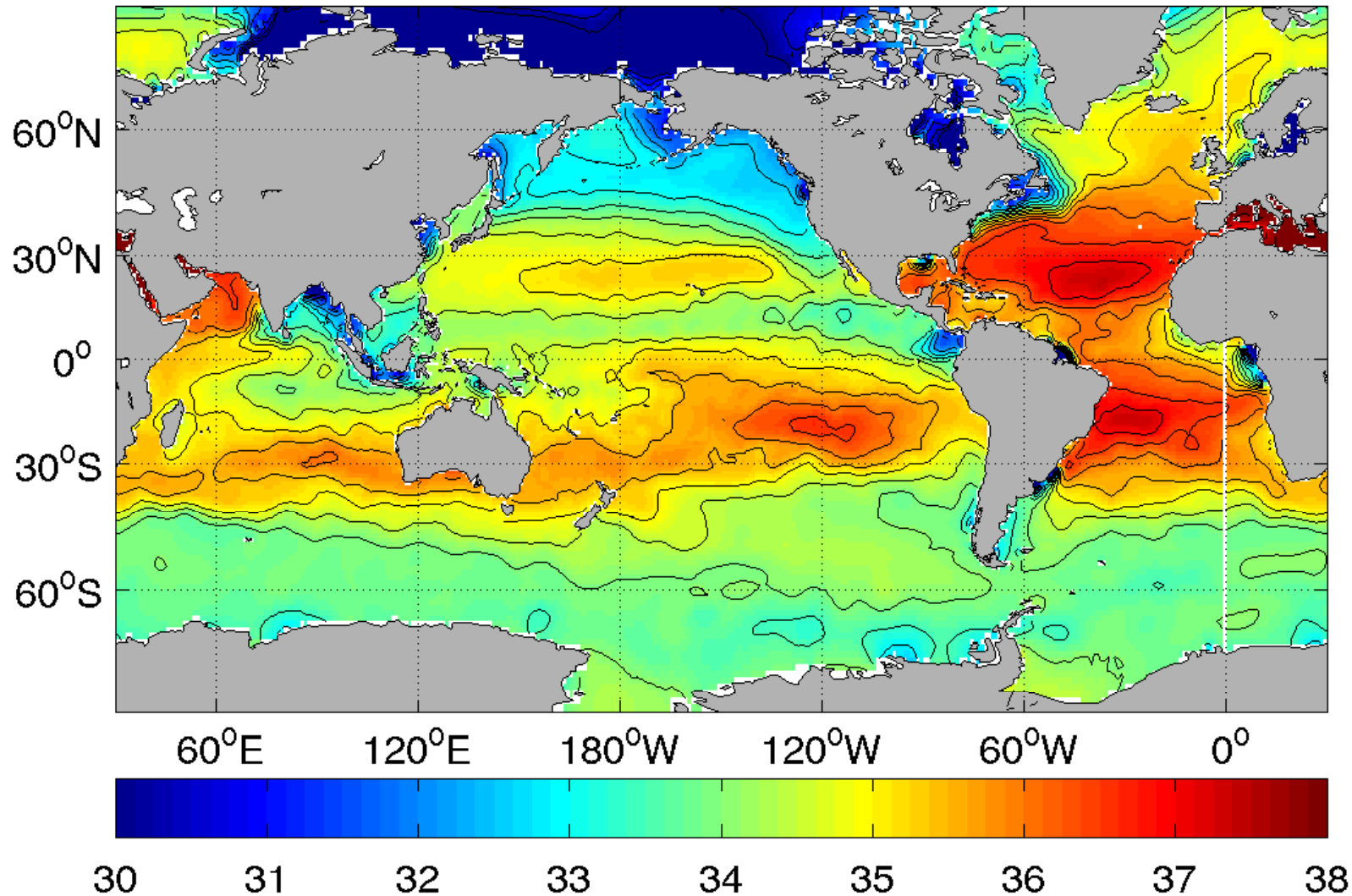
where  $\alpha, \beta > 0$ , and  $d\rho/dz < 0$  usually (with  $z$  upward).

Thus, there is gravitational inhibition for vertical motions, up or down.

Thus, the abyss is mostly isolated from the atmosphere except in polar regions where  $d\rho/dz$  is smaller and there are intermittent episodes of deep convection (deep-water formation) when  $d\rho/dz > 0$ .

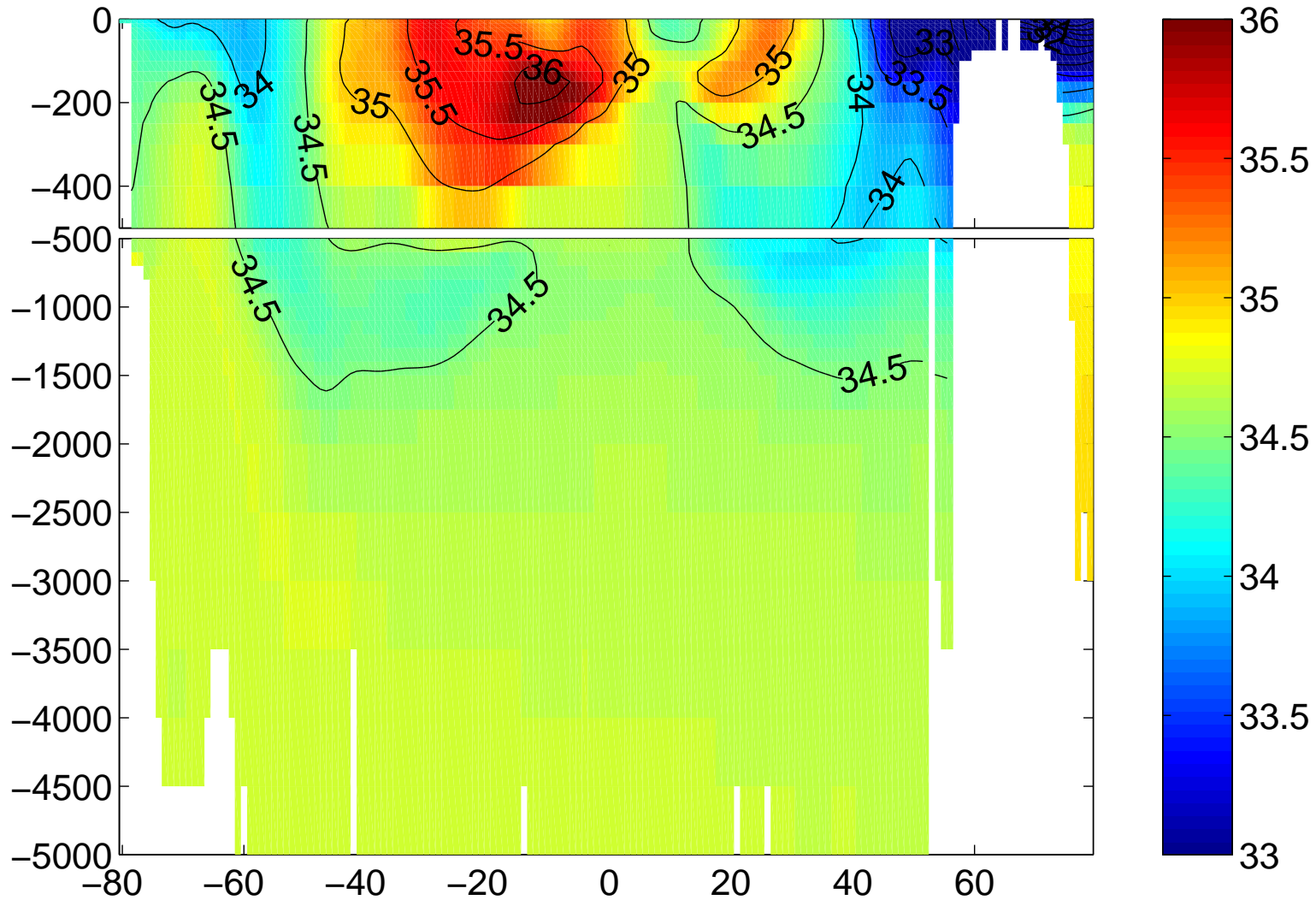


# Sea Surface Salinity



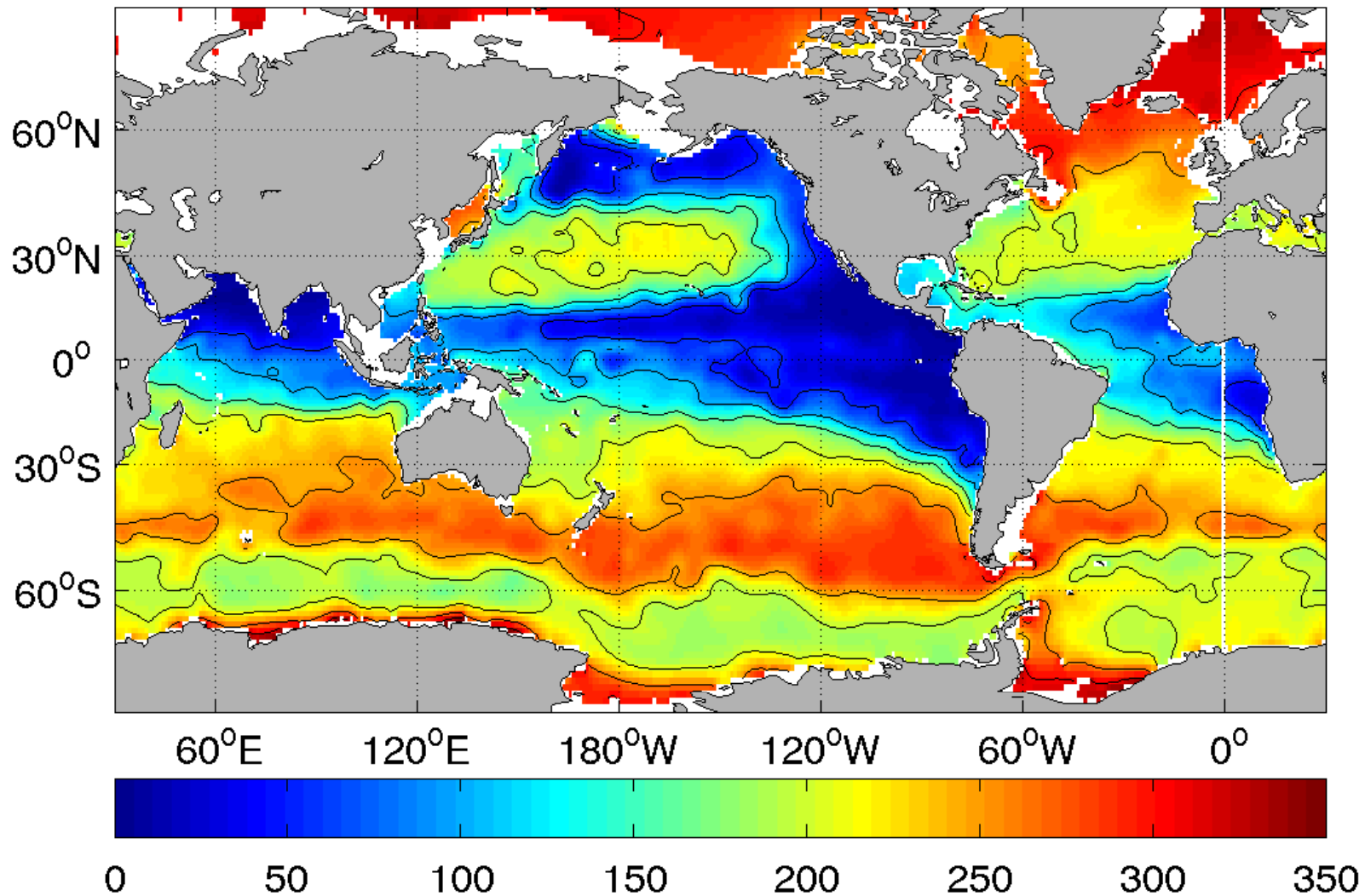
Annual mean salinity [ppt, PSU] at the surface (World Ocean Atlas, 2005). Salinity is a measure of the mass fraction of all the dissolved ions in seawater, most often measured with a CTD. The conductivity of seawater increases with the concentration of ions, so salinity can be measured from the electrical current through a sample. Surface salinity shows the influence of evaporation, precipitation, and runoff. Subtropics are saltier than polar regions, especially the Arctic.

## Salinity Section (Pacific)



Annual mean salinity  $S$ (latitude [ $^{\circ}$ N], depth [m]) [PSU] along 170W in the Pacific (World Ocean Atlas, 2005). Fresh water is lighter. The vertical gradient of  $S$  is the halocline. Like many oceanic materials (*e.g.*, T, O<sub>2</sub>, NO<sub>3</sub>, CO<sub>2</sub>), salinity variations show layer-like structures that trace back to distinct surface regions where the “water mass” is formed by air-sea flux then carried by the flow into the interior (*n.b.*, Antarctic and North Pacific Intermediate Water here). Many materials are only measurable from ships.

## Thermocline O2



Annual mean concentration of dissolved O<sub>2</sub> gas [ $\text{mmol/m}^3 = \mu\text{mol/liter} = \mu\text{M}$ ] at 400m depth (World Ocean Atlas, 2005). Dissolved oxygen is one of the most measured quantities in the ocean, albeit with limited precision, usually measured by a chemical titration (but see Argo). It reflects the combined effects of circulation and biogeochemical activity, with oxygen consumption (respiration, oxidation) in the interior. Low O<sub>2</sub> is where the vertical velocity  $w$  is mostly upward.



**Concept:** The ocean is chemically heterogeneous (much more so than the atmospheric troposphere).

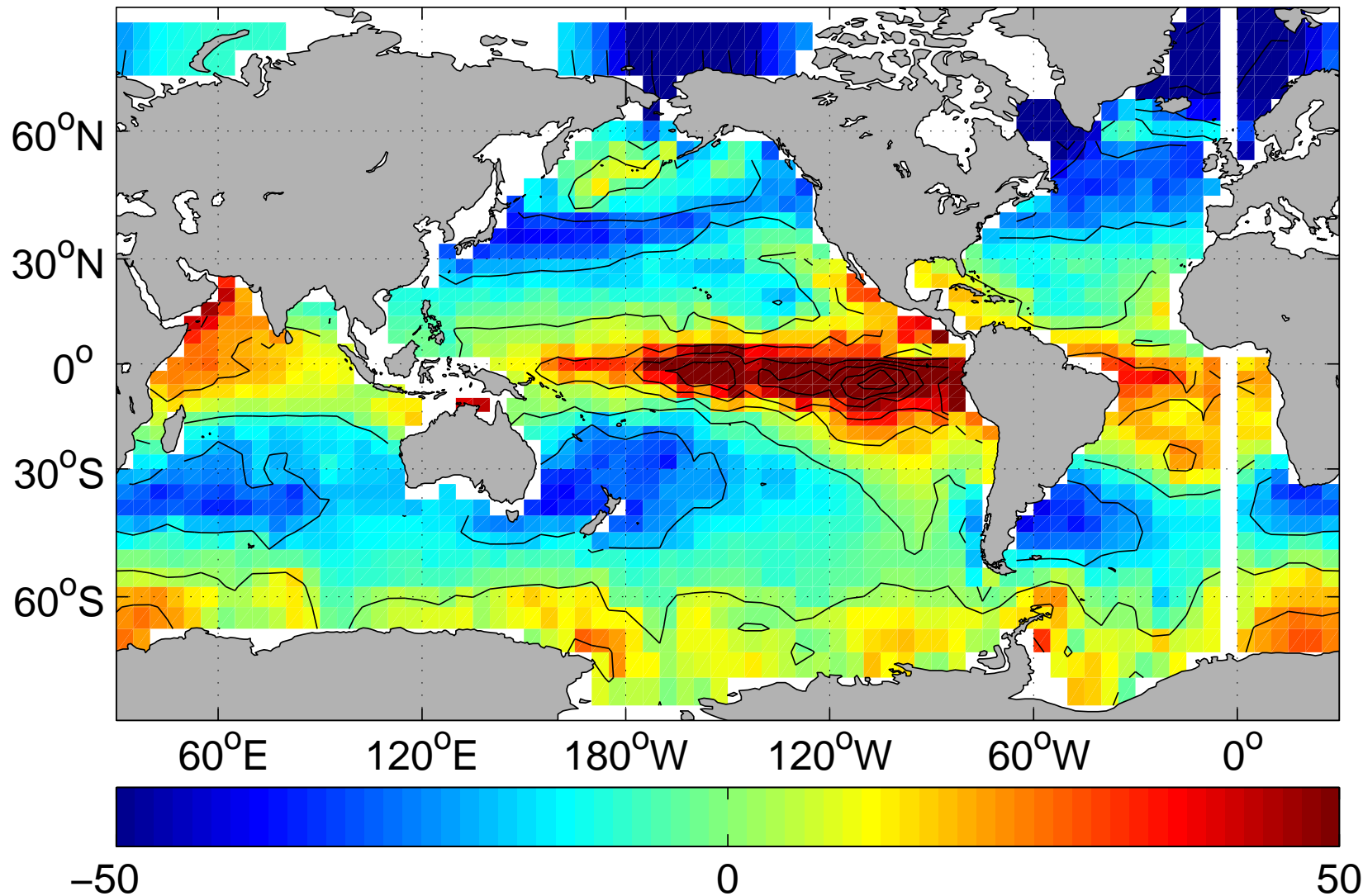
Physical transport (advection and mixing) strongly regulate the inhomogeneities.

Beneath the surface layer biogeochemical reaction rates are relatively slow (weeks to millennia).

Different “source” regions (water-mass formation sites) are well separated from each other in space and time, and their homogenization by mixing takes millennia.

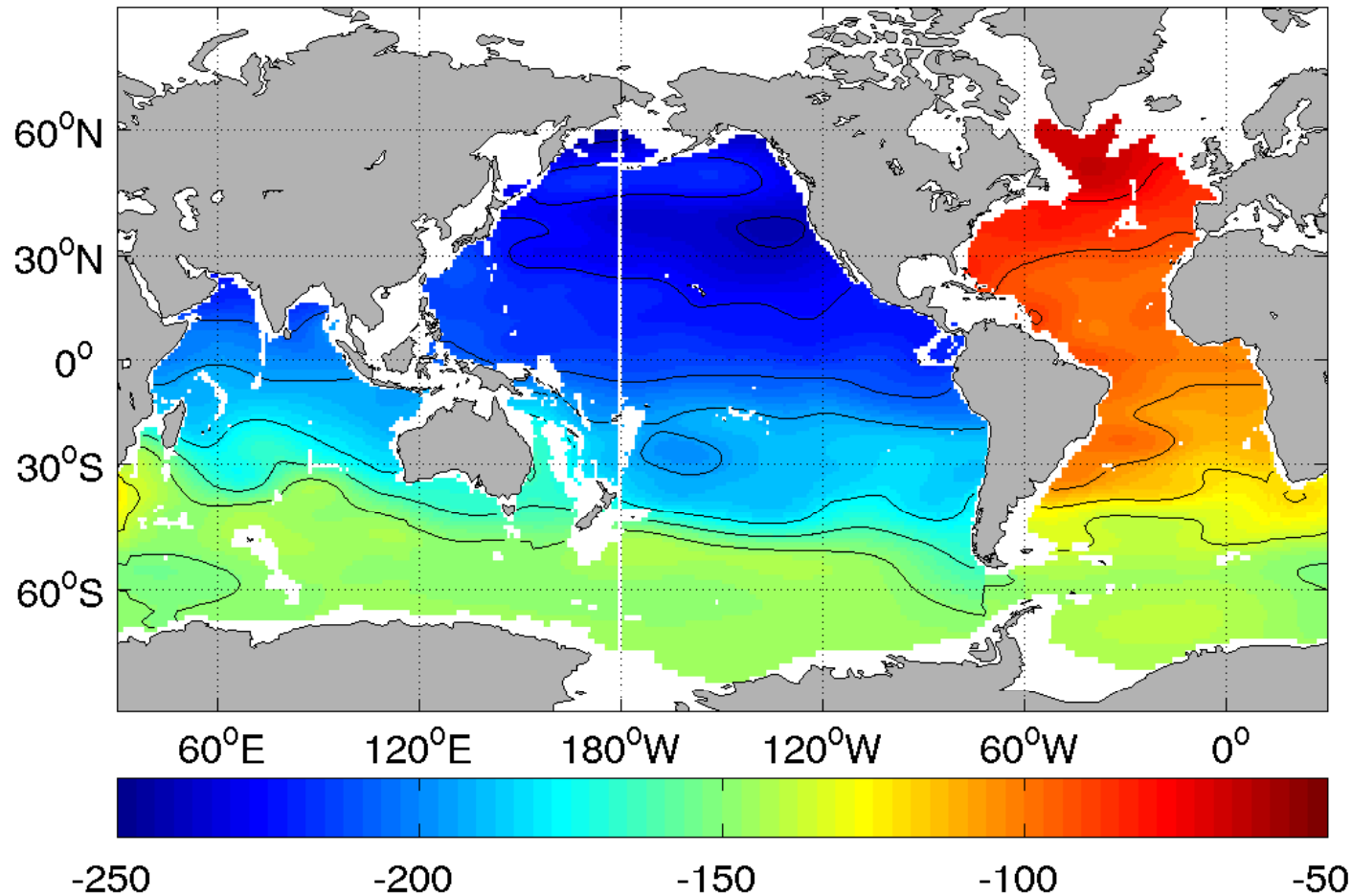
Photochemistry and photosynthesis are limited to the surface “euphotic” layer  $\sim 100$  m thick.

## Air-sea Delta pCO<sub>2</sub>



Annual mean air-sea difference in the partial pressure of CO<sub>2</sub> ( $\mu\text{atm} = 0.1 \text{ Pa}$ ). from the Takahashi database of nearly 2 million measurements, many from volunteer observation ships (VOS) [[http://cdiac.ornl.gov/oceans/LDEO\\_Underway\\_Database/LDEO\\_home.html](http://cdiac.ornl.gov/oceans/LDEO_Underway_Database/LDEO_home.html)]. The pattern drives large CO<sub>2</sub> exchange between the atmosphere and ocean, produced by variations in the pCO<sub>2</sub> of the surface ocean due to temperature, circulation, chemical composition, and biological activity.

# Deep Ocean Radiocarbon



Relative concentration of radiocarbon  $\Delta^{14}\text{C}$  [‰] in total inorganic carbon at 2500m depth. Measurements were made by decay counting and mass spectrometry during WOCE. Values are in per mil of normalized anomaly relative to a common atmospheric standard, Radioactive decay of  $^{14}\text{C}$  is a clock for time since cosmic-ray exposure at the surface for the abyssal circulation (with times up to about 1000 yr). The youngest and oldest waters are in the subpolar North Atlantic and Pacific, respectively, reflecting the global overturning circulation. Source: GLODAP (Global Ocean Data Analysis Project; <http://cdiac.ornl.gov/oceans/glodap/GlopDV.htm>).

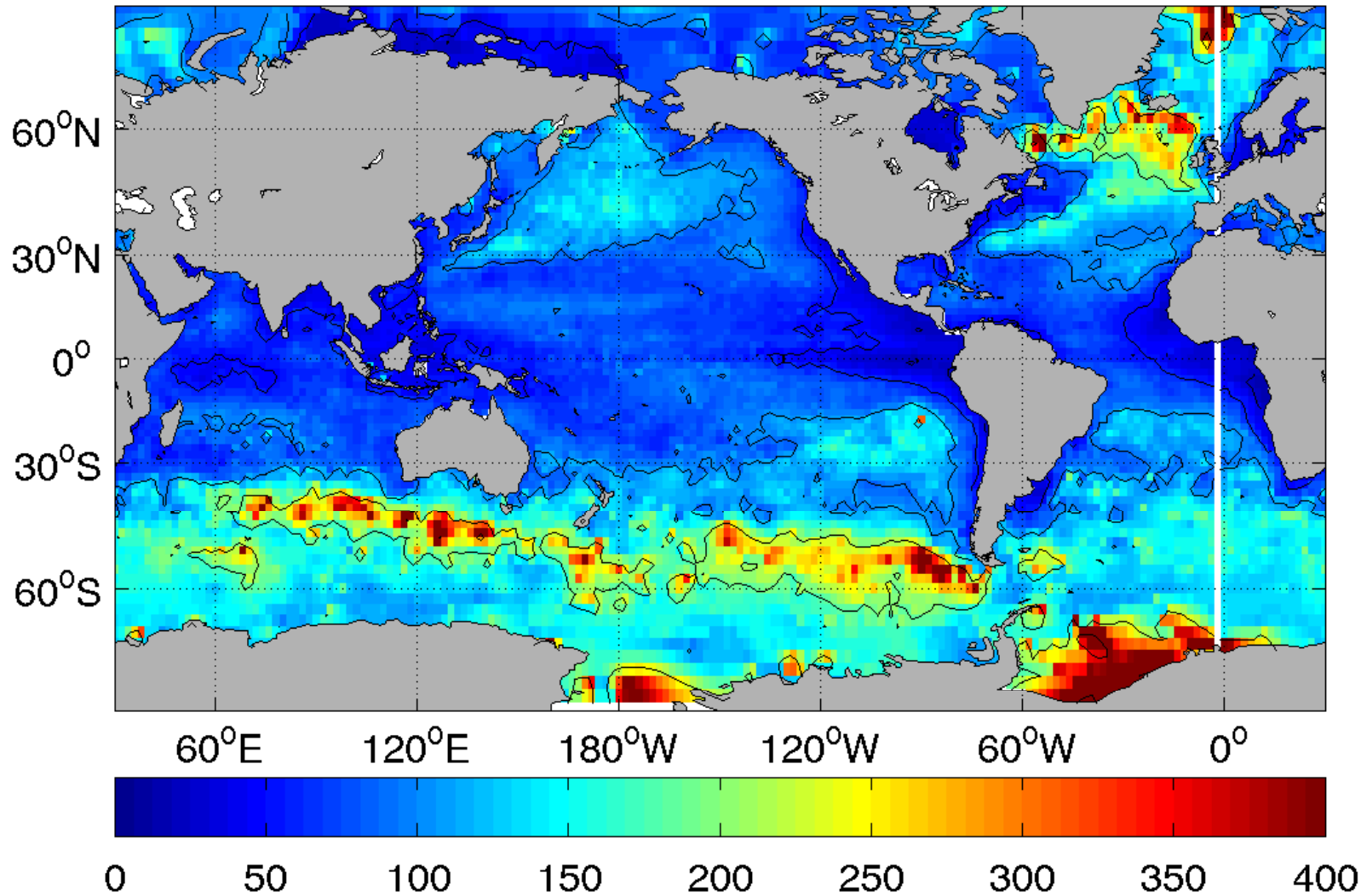


**Concept:** Material exchanges across the surface with the ocean have increasingly long time scales with depth in the ocean.

When a change in surface flux occurs, its depth of penetration into the ocean  $D$  depends on how long the flux change persists.

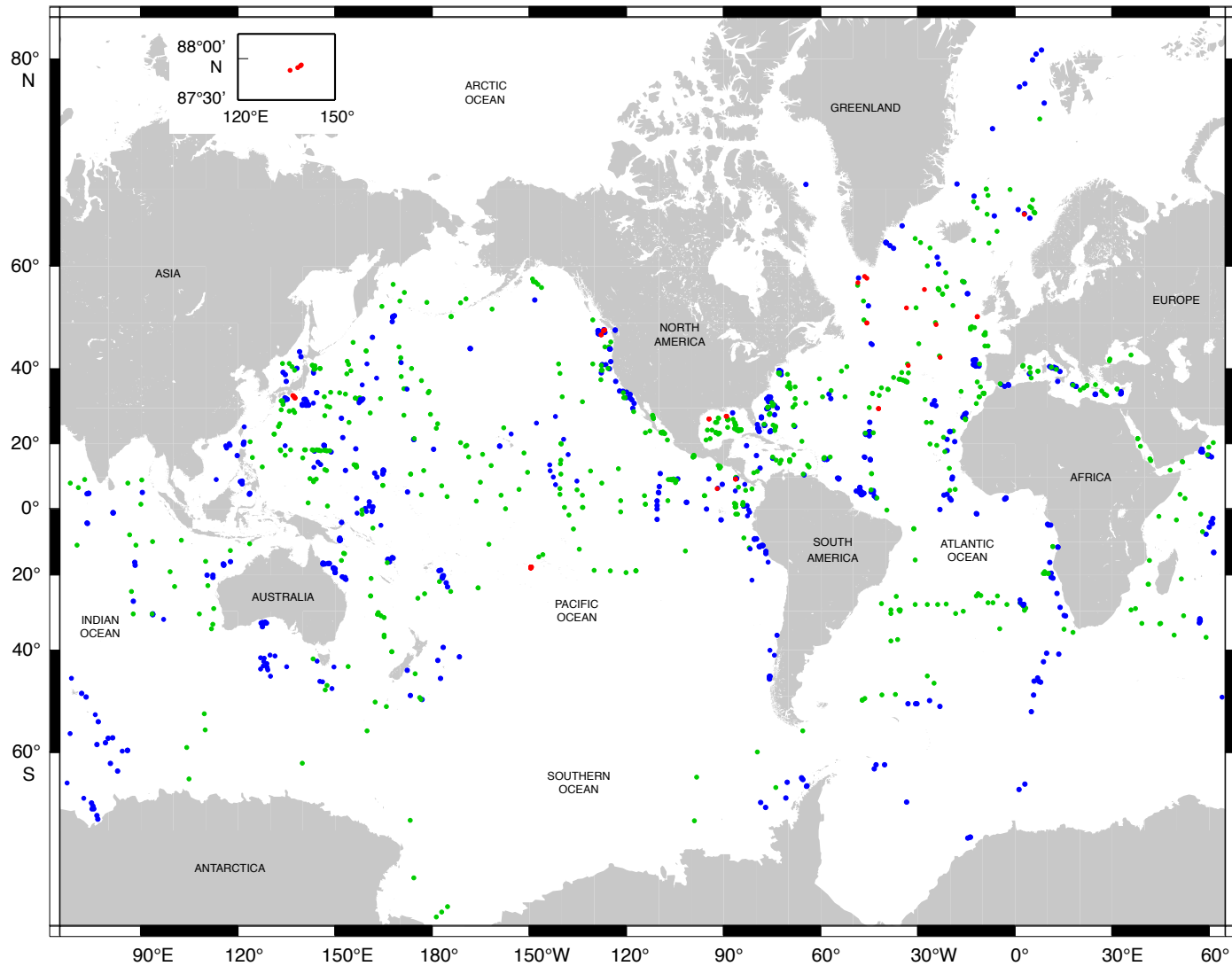
Within the surface (mixed) layer ( $D \sim 100$  m), surface-forced changes occur over diurnal to seasonal periods. In the “permanent” thermocline/pycnocline ( $D \sim 500$  m) changes occur over years to decades. In the abyss, ( $D \sim 5000$  m) changes occur over centuries to millennia (*e.g.*, ice ages).

## Mixed Layer Depth (MLD)



Maximum monthly mean depth [m] of the surface mixed layer, estimated from climatological profiles of  $T$ ,  $S$  (de Boyer *et al.*, 2004). The mixed layer is operationally (and variously) defined as the depth to which turbulence mixes the density in the boundary layer. It indicates regions of vigorous exchange between the atmosphere and surface waters. MLD is large where surface waters are dense, winds are strong, and/or stratification is weak.

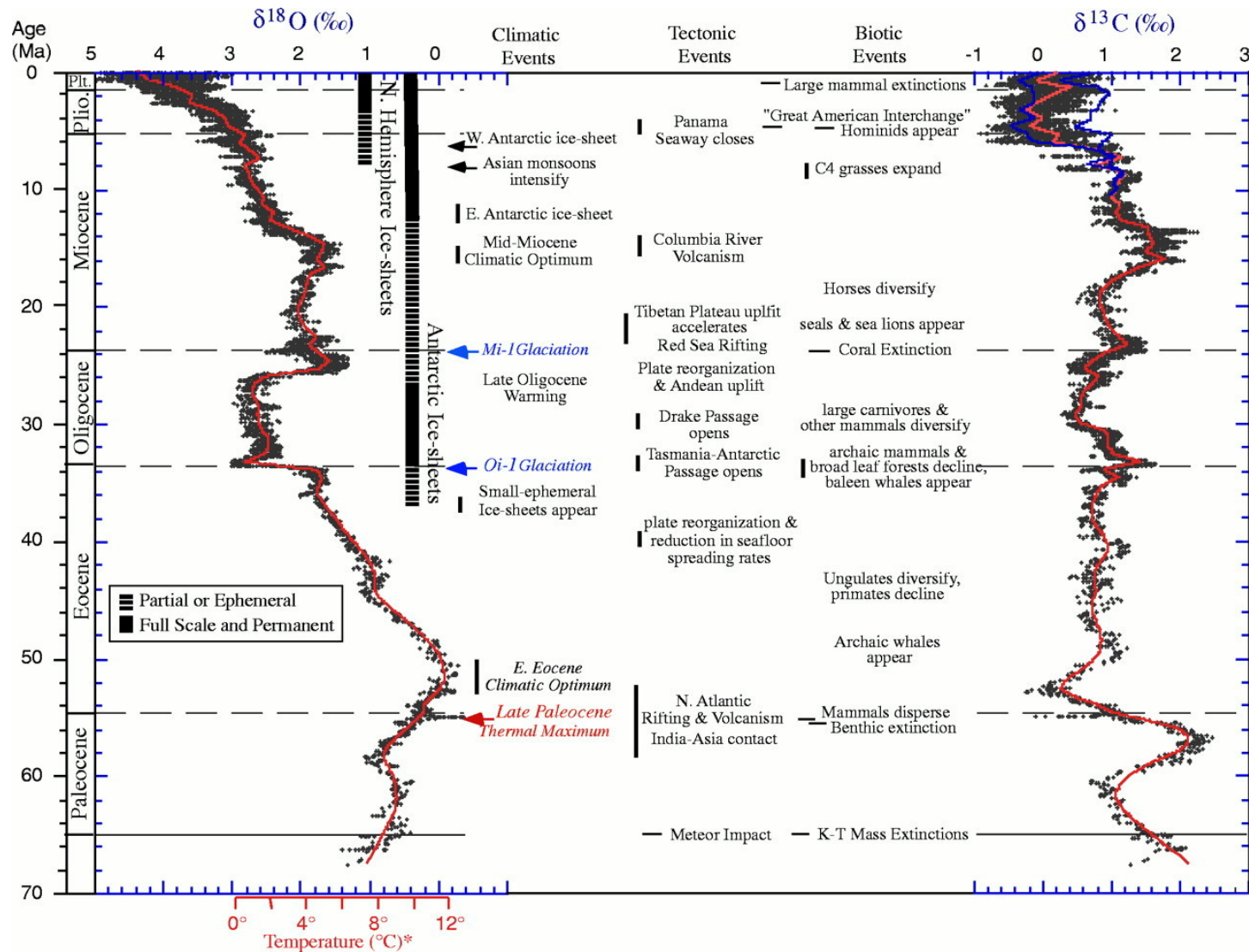
# Sediment Cores



DSDP Legs 1–96 (●), ODP Legs 100–210 (●), IODP Expeditions 301–312 & 314–316 (●)

Locations where sediment cores have been extracted by the Ocean Drilling Program and its relatives. Cores and data are archived in storage facilities around the world (<http://www.iodp.org/>). Sediments provide a chemical and biological history with increasing burial as solid material is deposited from above.

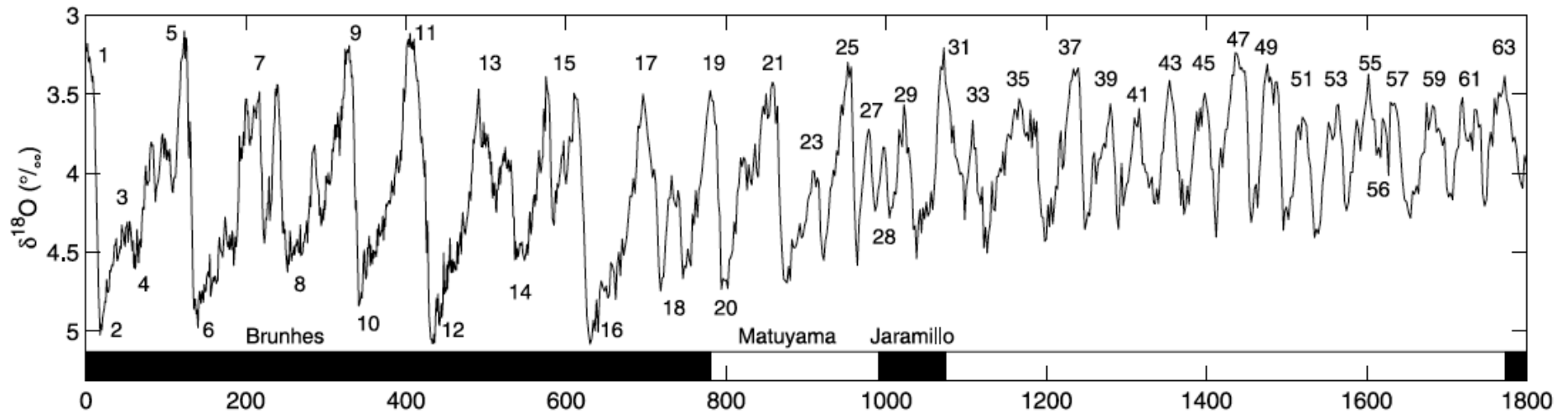
# Earth History to 65 Myr



Sedimentary isotope ratios of carbon ( $^{13}\text{C}/^{12}\text{C}$ ) and oxygen ( $^{18}\text{O}/^{16}\text{O}$ ) in  $\text{CaCO}_3$  shells of plankton, measured by mass spectrometry (Zachos *et al.*, 2001). These are among the best proxies of past climate. Prior to the large glaciations in the past 35 Myr (Ma),  $\delta^{18}\text{O}$  is a proxy of ocean  $T$ ; afterward it measures the combination of  $T$  and oceanic volume (land glaciers and sea level).  $\delta^{13}\text{C}$  mostly reflects carbonate exchange with sediments.



# Glacial - Interglacial Cycles

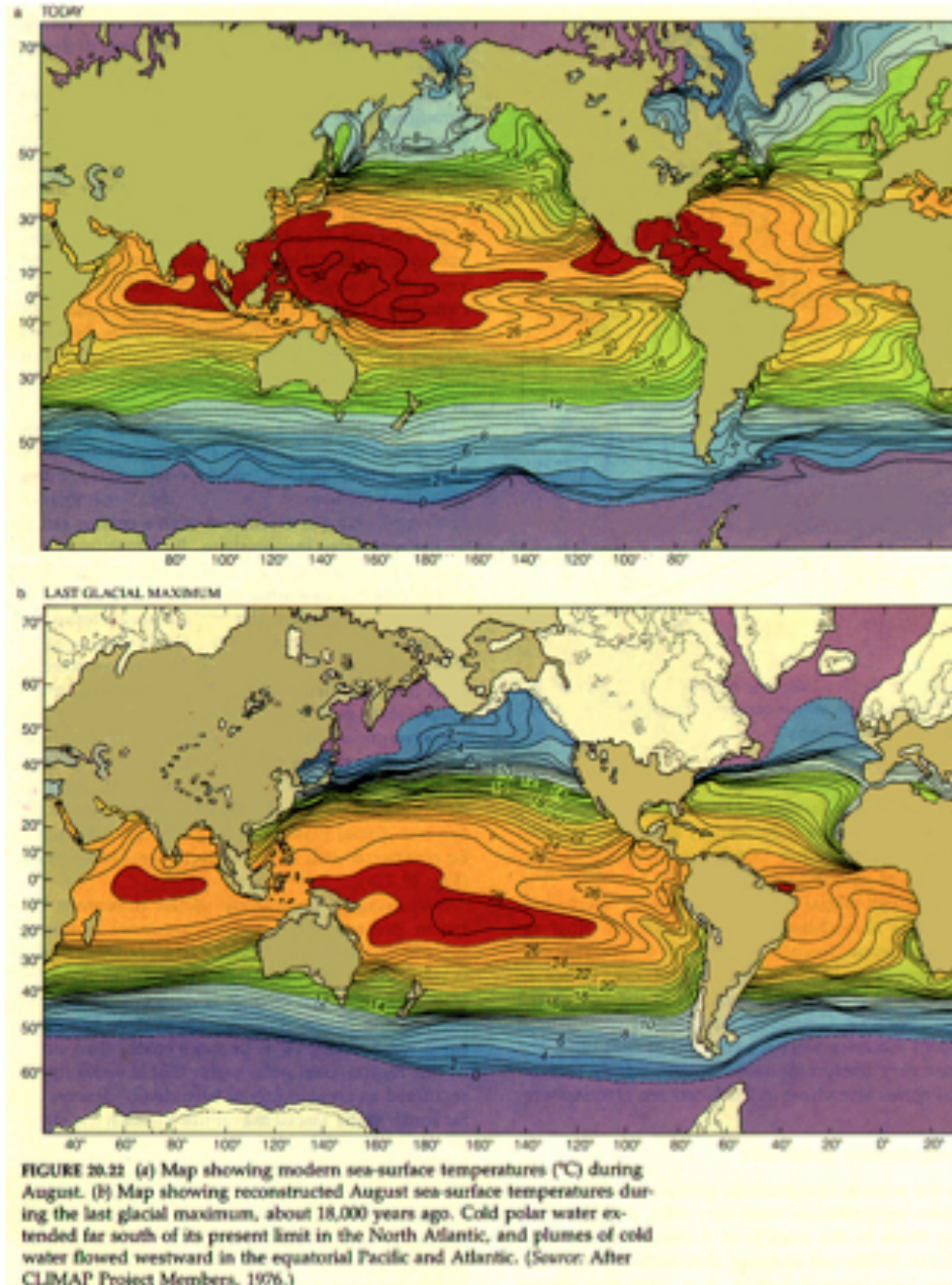


The isotope ratio of oxygen ( $^{18}\text{O}/^{16}\text{O}$ ) in  $\text{CaCO}_3$  shells of plankton, measured by mass spectrometry. This compilation of numerous sediment cores shows the glacial-interglacial cycles of the past 1800ky (most of the Pleistocene epoch). The instigations for such oscillations are the Milankovich cycles of seasonal insolation distribution changes, although the climate response is far from a simple mirror of the astronomical forcing. Note the change in power from  $\sim 40\text{ky}$  (axis tilt) before 1200 ky to  $\sim 100\text{ky}$  (orbit eccentricity) afterward, which is still a dynamical mystery.

**Concept:** Deep-time changes in the ocean ( $> 10^4$  years) coincide with deep-time changes in climate, and they both are due to “external” influences: solar insolation, atmospheric composition, plate movements, and biological evolution (“Gaia”).

$10^4$  years is essentially a complete oceanic mixing time over the full volume.

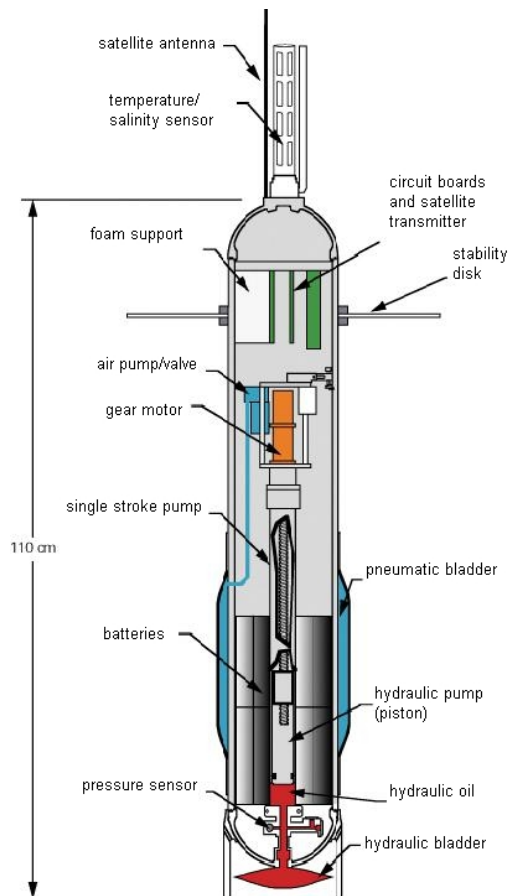
# Paleoclimate Temperatures



Surface temperature comparisons between the Last Glacial Maximum (LGM; bottom), about 23 ky ago, and the modern era (top).

CLIMAP was a major research program in the 1970s to reconstruct the glacial climate at the LGM by means of fossil evidence from ocean sediment cores. Shown here is the reconstruction of sea surface temperatures. More recent evidence indicates SSTs were 2-5 C cooler in the tropics in the LGM.

# Autonomous Platforms



## Pros/Cons:

High resolution in space and/or time  
Limited process studies  
Relatively inexpensive  
Limited measurement capacity

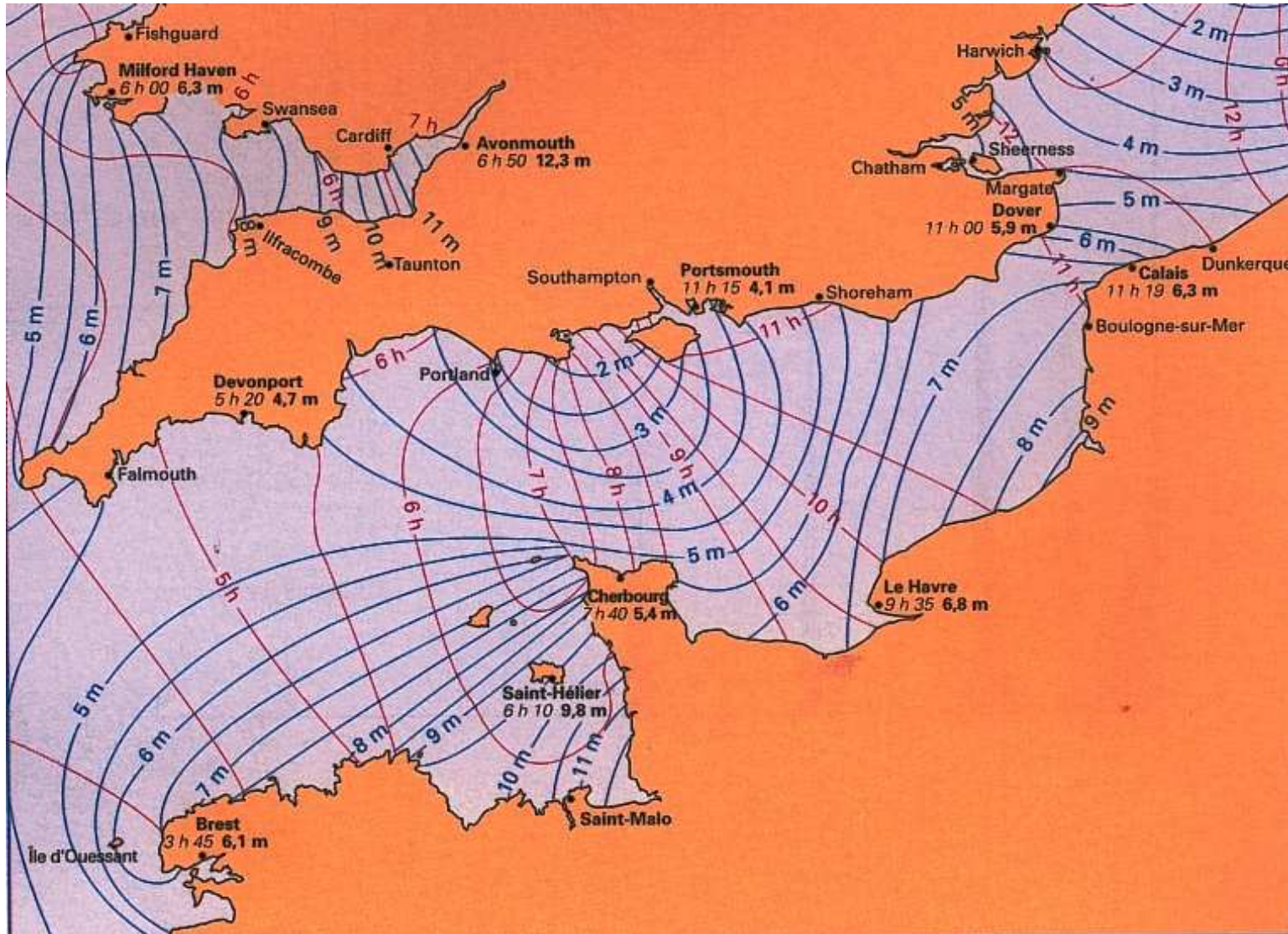
## Key Results:

Surface currents  
Wave spectra  
Time series  
Hydrography

The future of oceanic measurements beneath the surface is potentially brighter with better designed and more abundant autonomous platforms *faute de mieux*. Difficulties are lifetime, range, cost, sensor varieties, and data communication bandwidth. Examples here are a vertically cycling profiler and a surface buoy with air and water sensors and solar panels. Data transmission is either acoustic through the interior or by satellite relay from the surface.



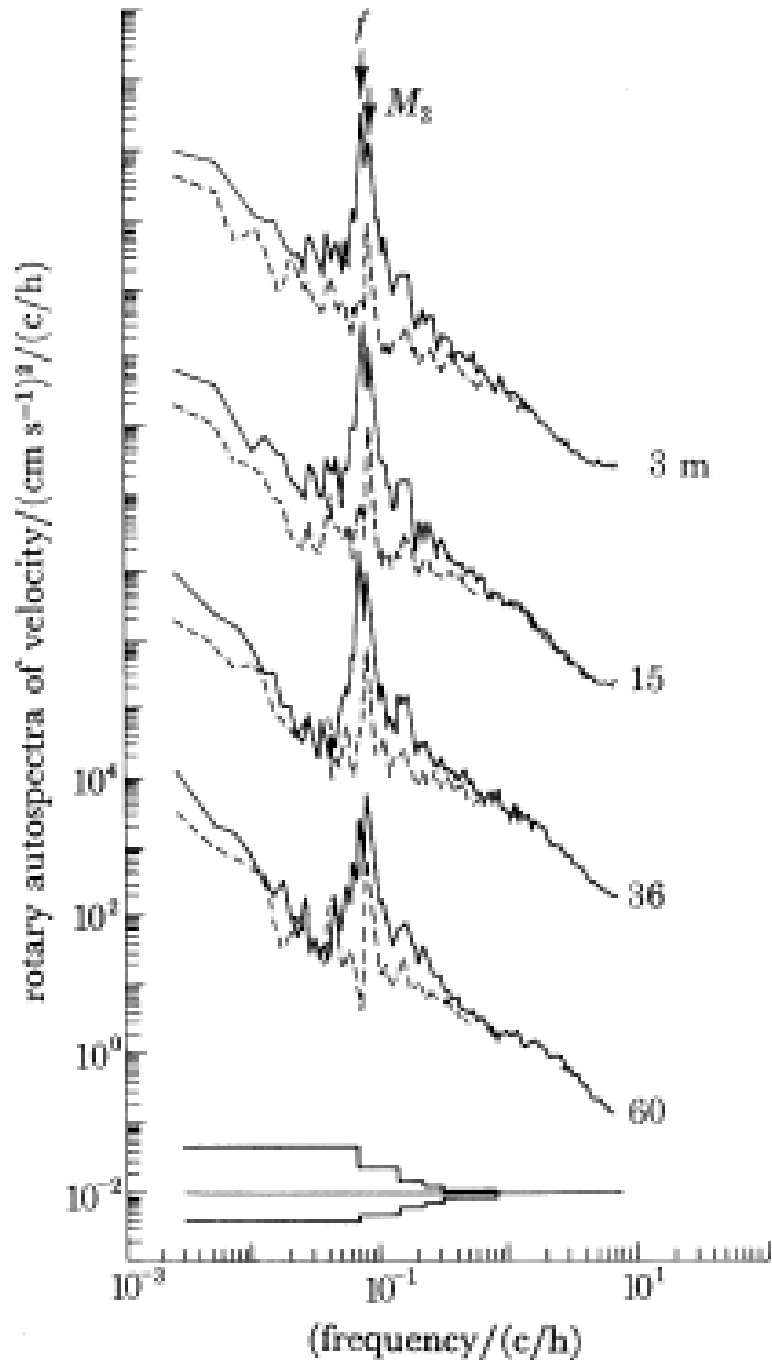
# “Tide” Gauges



Barotropic (*i.e.*, full-depth velocity) tides: regional sea level amplitude [m] (peak-to-trough) and phase [hours in a cycle] of the M2 (lunar semi-diurnal) tide around the English Channel determined mainly from unattended coastal tide gauges (SHOM, 1997). Over the broader ocean sea level measured by satellite altimetry is a better alternative. Mariners beware!



# Moorings: Oceanic Frequency Spectra



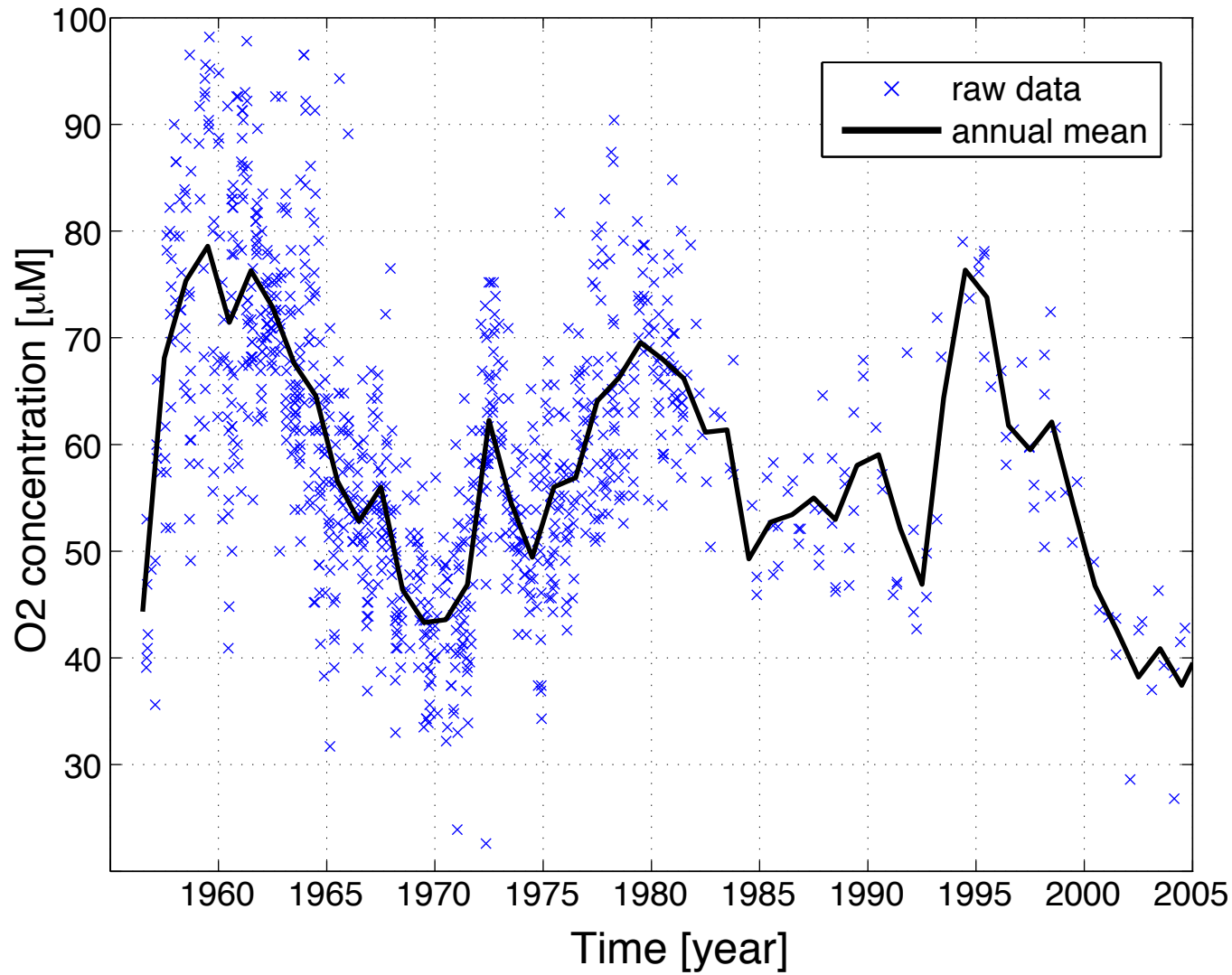
Moored current meter time series: rotary autospectra of horizontal velocity at 3, 15, 36 and 60 m at a site in the northeastern Atlantic Ocean. Confidence limits (95 %) are shown below the spectra. The solid lines are the clockwise ( $\omega < 0$ ) spectra, and the dashed lines are the counterclockwise ( $\omega > 0$ ) spectra. The 3, 15, and 36 m spectra are plotted three decades above the spectrum from the next deepest record. The spectrum peaks are at tidal and Coriolis frequencies; higher frequencies are mostly internal waves, and lower frequencies are mostly mesoscale eddies and response to low-frequency atmospheric forcing. (Weller and Halpern, 1983)

**Concept:** Variable currents are the norm in the ocean.

Time- or volume-averaged currents are much weaker than instantaneous ones. This is especially true for the vertical current  $w$ .

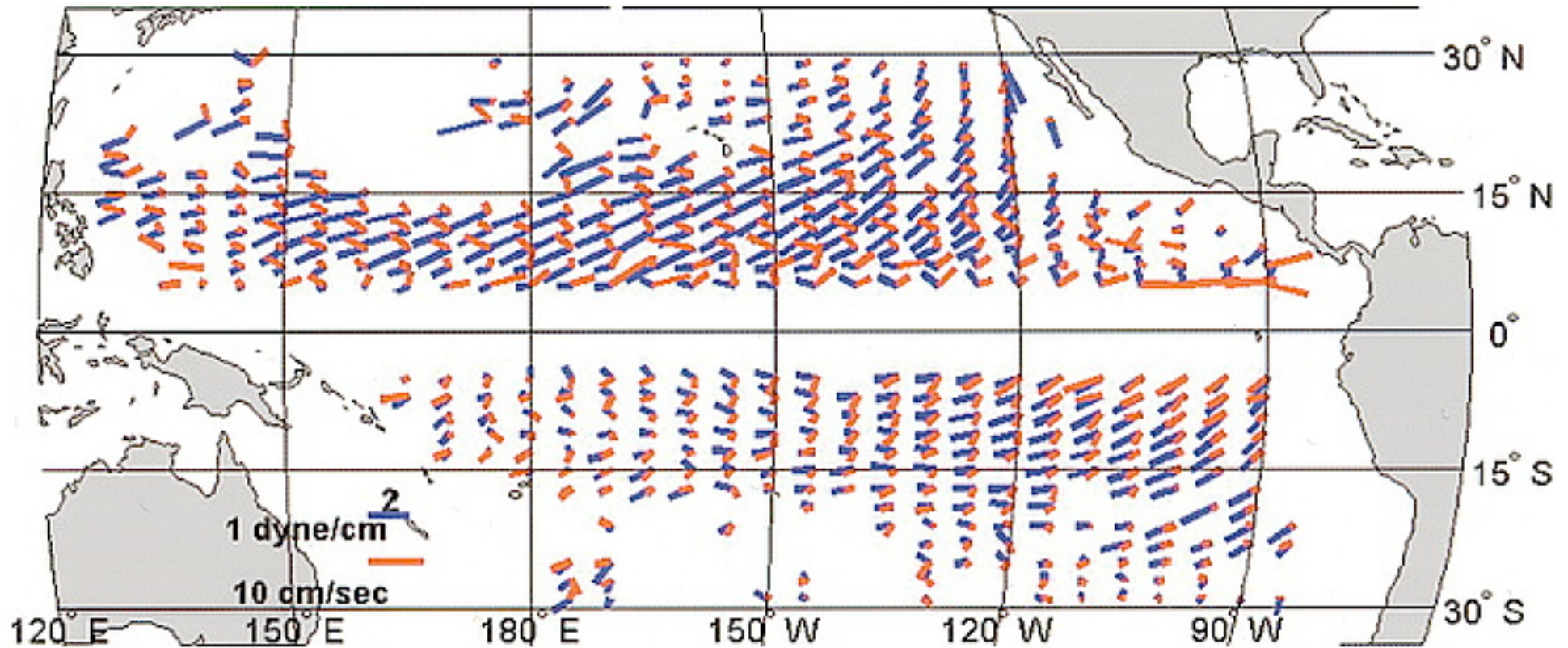
The causes and types of variability are multiple, and they include both atmospherically and tidally forced variations and spontaneous ones (often called waves or eddies).

# Hydrographic Time Series: Oxygen



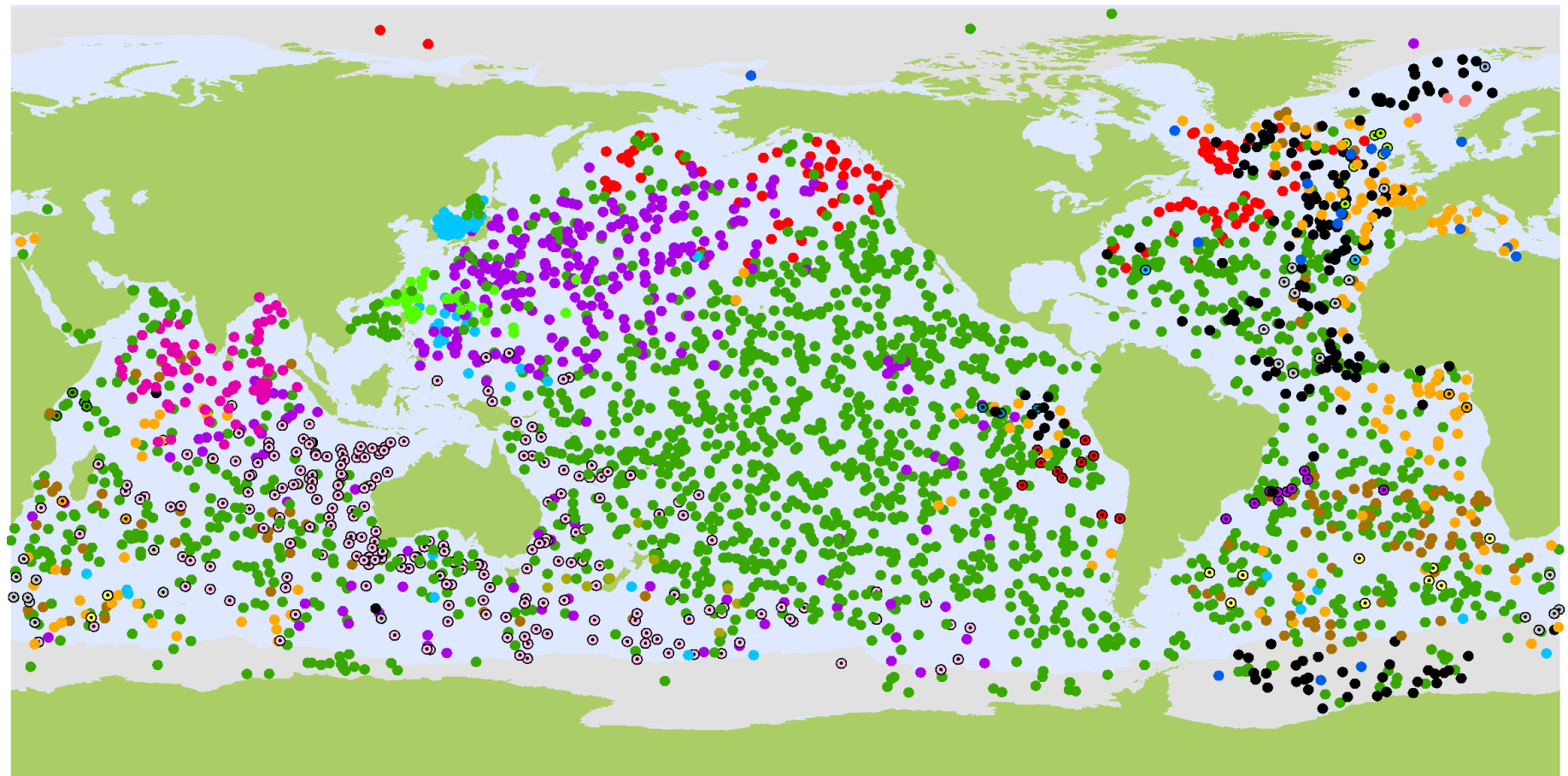
Time series of oxygen [ $\mu\text{M} = \text{mmole}/\text{m}^3$ ] measurements (blue) and their annual mean values (black) from bi-weekly ship cruises starting in the 1950s [Whitney *et al.*, 2007]. These are sampled on an interior isopycnal ( $\rho$ ) surface (North Pacific Intermediate Water  $\sim 350$  m deep). Decadal variability is evident. Long-term trends and low-frequency variations are directly observable from only a few such time-series stations. Notice the sparser sampling after 1980.

## Drogued and Tracked Drifters: Surface Currents



Mean wind stress [blue;  $\text{dyne cm}^{-2} = 0.1 \text{ N m}^{-2}$ ] and surface current [red;  $\text{cm s}^{-1} = 0.01 \text{ m s}^{-1}$ ] in the tropical Pacific. Note the tendency for Ekman (boundary layer) flow to the right or left of the wind in the Northern or Southern Hemisphere, which implies a surface divergence near the equator with compensating upwelling from the interior. The tropical winds are the Trade Winds, and the tropical currents are a combination of Ekman (mostly meridional) and geostrophic-hydrostatic (mostly zonal). (Ralph and Niiler, 1999)

# Floats: ARGO network



3261 Argo Floats

○ ARGENTINA (11)	● CHINA (31)	● GERMANY (177)	● SOUTH KOREA (90)	○ POLAND (1)
○ AUSTRALIA (224)	● ECUADOR (3)	● INDIA (72)	● MAURITIUS (2)	● RUSSIAN FEDERATION (2)
● BRAZIL (10)	● EUROPEAN UNION (17)	● IRELAND (7)	○ NETHERLANDS (25)	● SPAIN (2)
● CANADA (118)	● FRANCE (156)	● JAPAN (320)	● NEW ZEALAND (9)	● UNITED KINGDOM (115)
● CHILE (10)	● GABON (2)	● KENYA (4)	● NORWAY (4)	● UNITED STATES (1849)

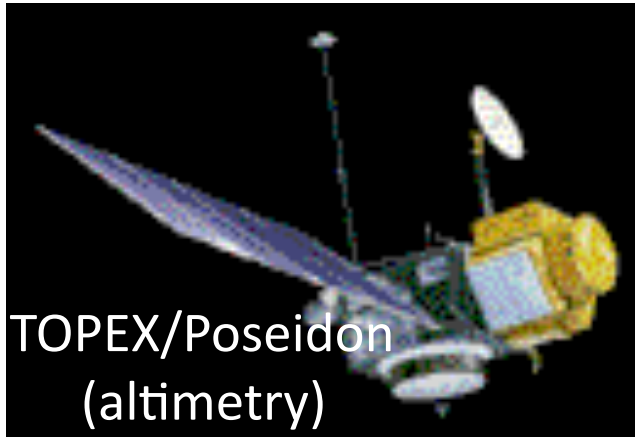
September 2009



Locations of the network of Argo floats, as of September, 2009. The floats are equipped with CTDs (and sometimes other sensors) and drift with the oceanic currents at different depths, surfacing at regular intervals ( $\sim 10$ -day) to measure vertical profiles and relay data via satellite. In addition to standard CTD data, the drift between profiles gives a measure of mean current at the parking depth. Argo profiles and sea level change are the primary ways to detect global warming in the ocean.



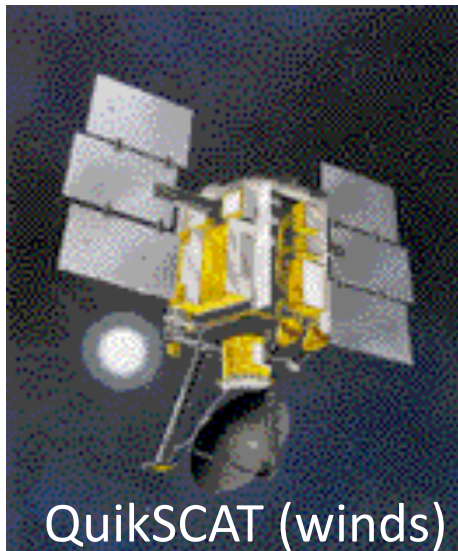
# Satellite Remote Sensing



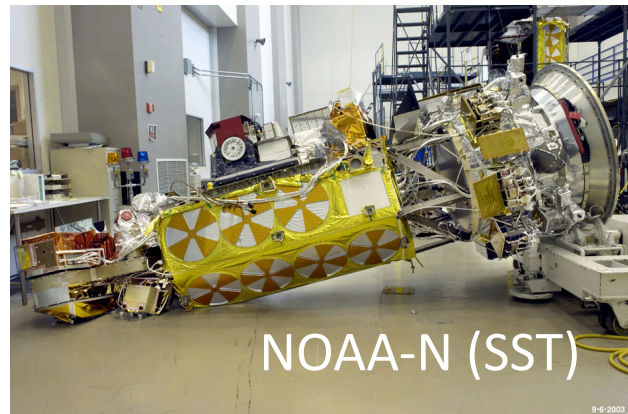
TOPEX/Poseidon  
(altimetry)



SeaWiFS (color)



QuikSCAT (winds)



NOAA-N (SST)

## Pros/Cons:

High resolution in space and/or time  
Surface ocean only  
Indirect measurements

## Key Results:

Surface temperature  
Surface chlorophyll  
Sea surface height

Satellites have greatly expanded the oceanic data base over the past few decades. [“I consider [altimetry] the most successful ocean experiment of all times” (Walter Munk, 2002).] Better sensors are possible in future, but the danger is a shortage of space missions, especially in the U.S.

International cooperation is essential.

# Satellite Orbits

**1. Geostationary orbit.** The satellite orbits in the same direction as the Earth with a period of one day. It is positioned in a circular orbit above the equator. Therefore, it becomes stationary relative to the Earth and always views the same area of the Earth's surface.

**2. Polar orbit.**  $i$  (inclination)  $\cong 90^\circ$ . Usually these satellites have height between 500 and 2,000 km and a period of about 1 to 2 hours. As the Earth rotates under this orbit the satellite effectively scans from north to south over one face and south to north across other face of the Earth, several times each day, achieving much greater surface coverage than if it were in a non-polar orbit.

**3. Sun-synchronous orbit.** The satellite crosses the equator at the same local solar time on each pass throughout the year. In practice  $i$  is about  $100^\circ$ , i. e., the orbit is not polar, but nearly polar.

## Satellite Sensors

### Passive sensors

Visible wavelength radiometers

Wavelength

400 nm - 1  $\mu\text{m}$

Information

Solar radiation reflected by Earth surface

Infrared (IR) radiometers

about 10  $\mu\text{m}$

Thermal emission of the Earth

Microwave radiometers

1.5 - 300 mm

Thermal emission of the Earth in the microwave

### Active devices

Altimeters

3 - 30 GHz

Earth surface topography

Scatterometers

3 - 30 GHz

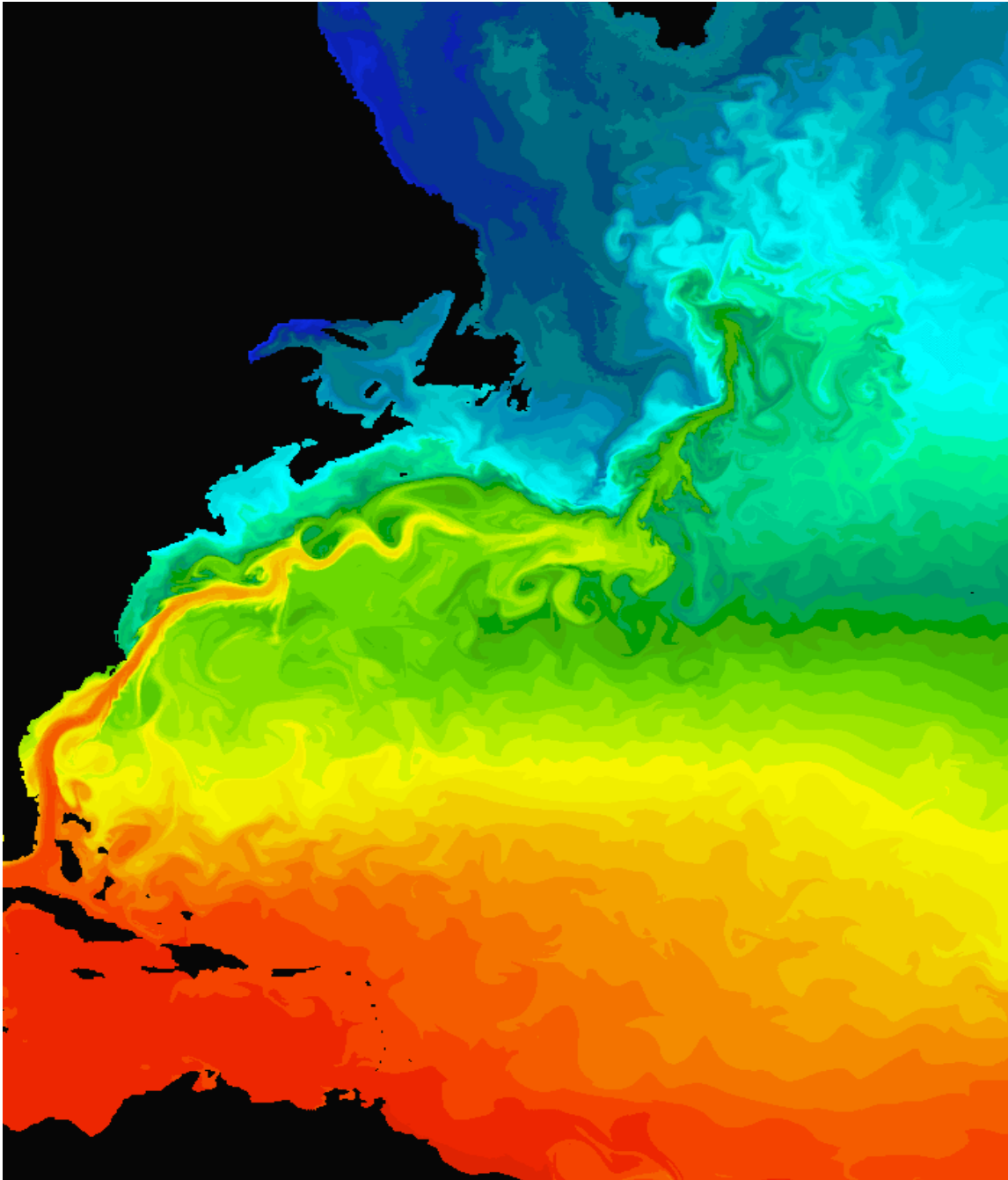
Sea surface roughness

Synthetic aperture radars

3 - 30 GHz

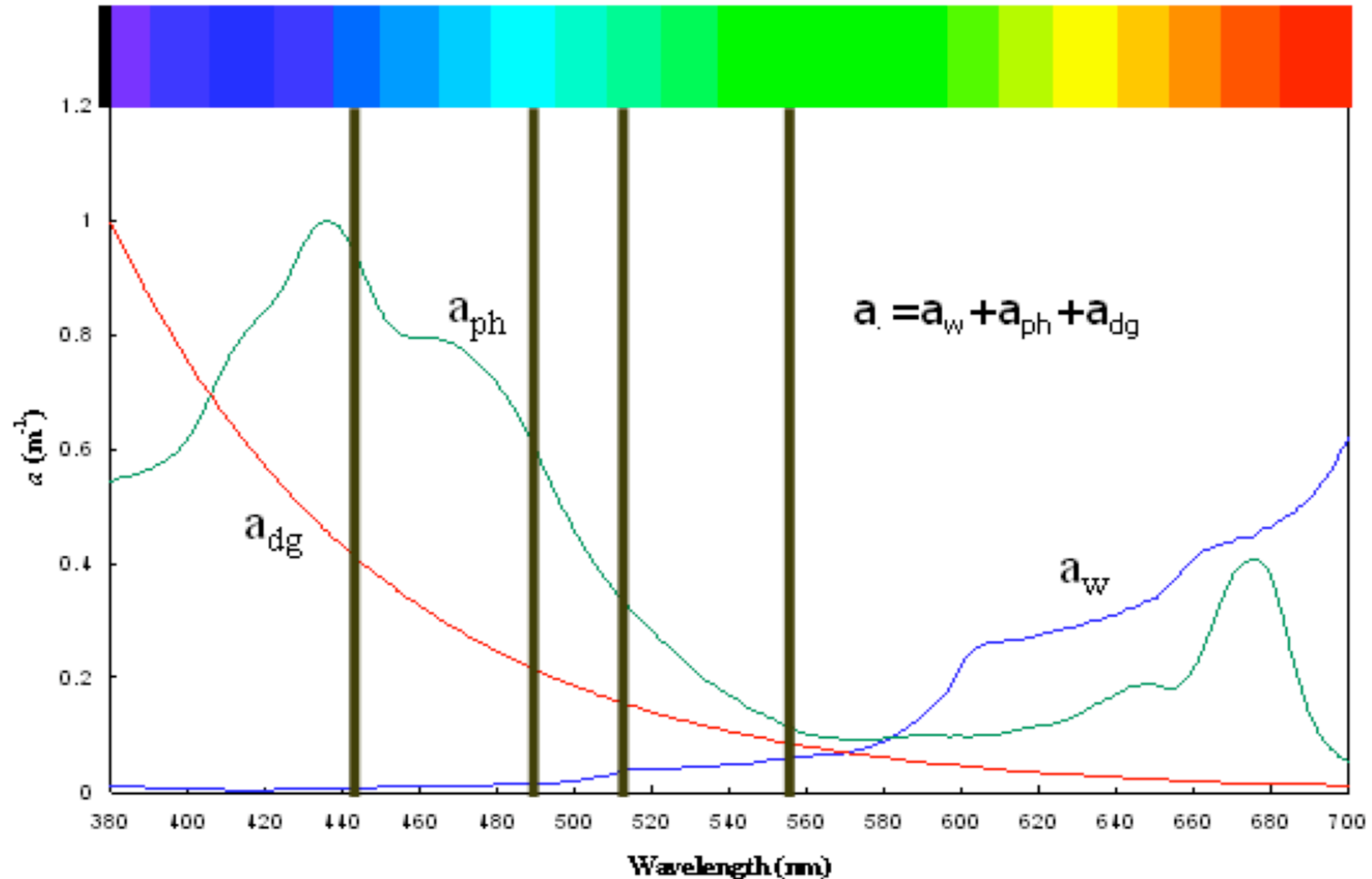
Sea surface roughness and movement

## Radiometry: High Resolution SST



Instantaneous pattern of SST in the western North Atlantic off the east coast of North America. SST is derived from thermal emission in the infrared band ( $\sim 12 \mu\text{m}$ ). The warm Gulf Stream and its mesoscale meanders are evident, along with the more broadly increasing SST with latitude. Mesoscale eddy fluctuations on a scale  $\sim 100\text{km}$  are widespread, though strongest near the Gulf Stream. Notice the cold boundary currents westward around the tip of Greenland and southward along the coast of Canada.

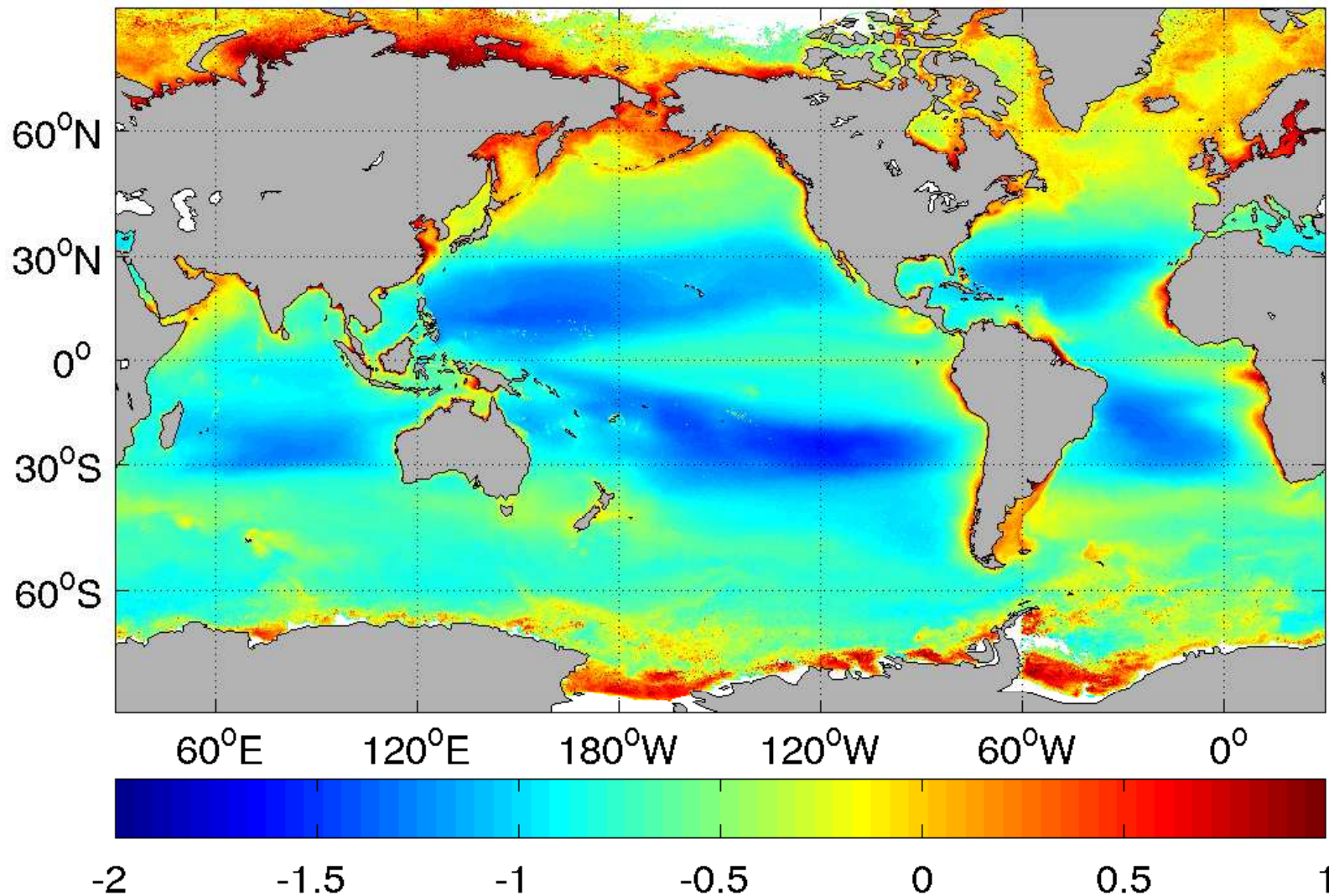
# Ocean Color



The absorption spectrum of seawater  $a_w$ , phytoplankton  $a_{ph}$ , and gelbstoff  $a_{dg}$  (yellow muck comprised of dissolved organic materials, DOM).  $a$  is inverse optical depth. After correcting for atmospheric absorption, the ratios of reflectances in different color bands (black lines) are used to estimate the presence of photosynthetic pigments (primarily chlorophyll-a) and, in coastal zones, dissolved organic matter.

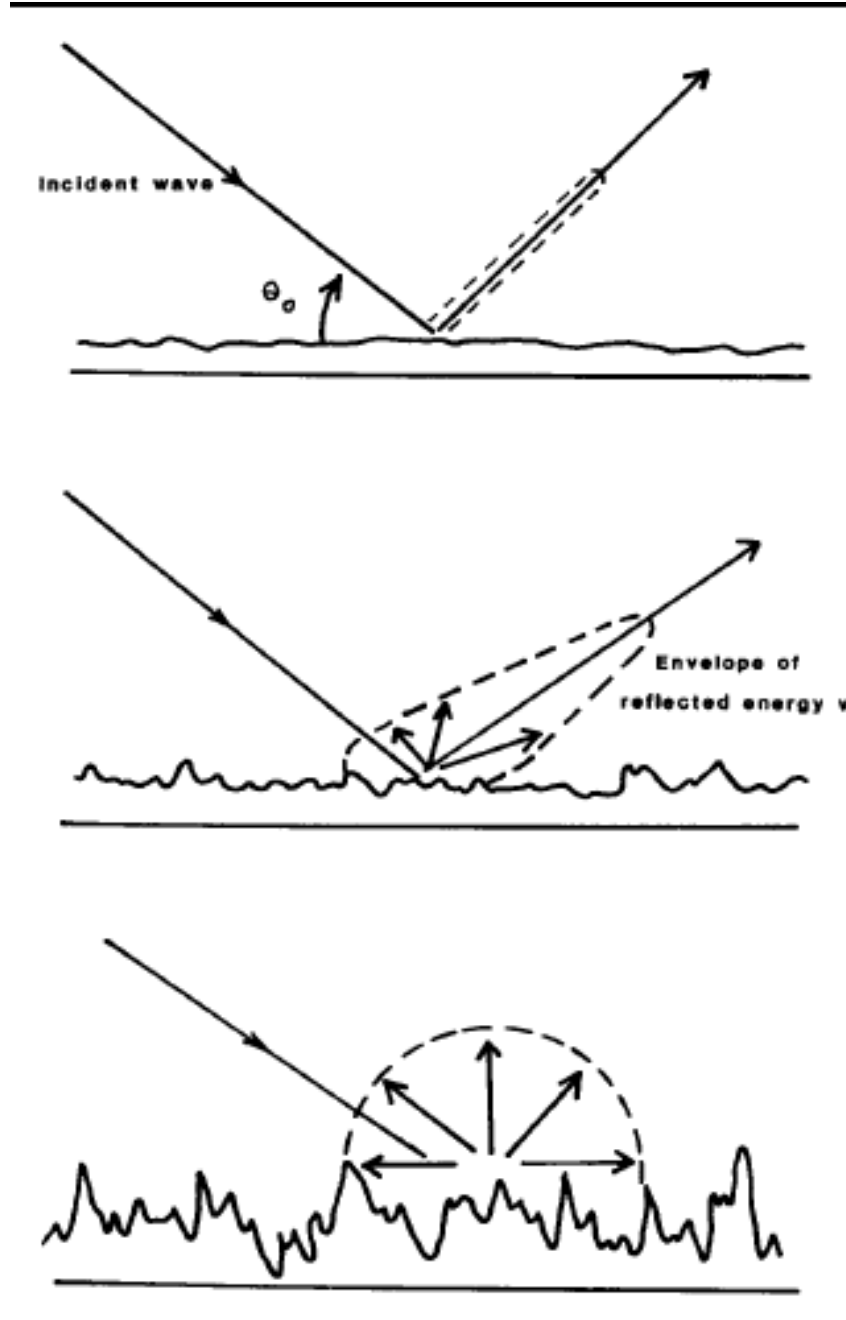


## Ocean Color: Chlorophyll



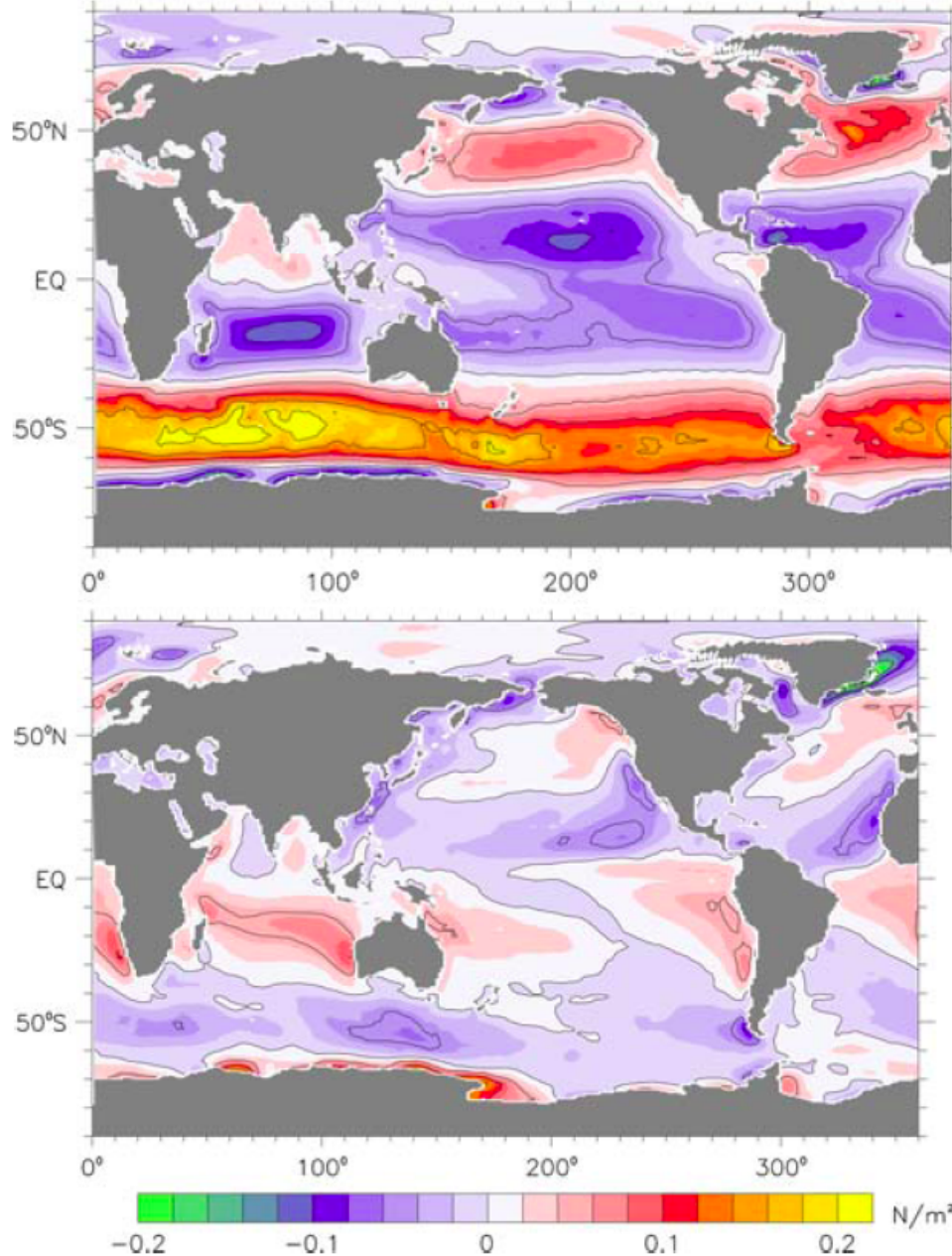
Annual average chlorophyll concentration [ $\text{mg m}^{-3}$ , log scale] from 1997-2005, according to the SeaWiFS satellite ocean color sensor. [<http://oceancolor.gsfc.nasa.gov/SeaWiFS/>]. The chlorophyll concentration is a rough measure of plankton abundance. Coastal and polar zones are especially productive because of higher nutrient supply from circulation, vertical mixing, sediment recycling on shelves, and run-off. Subtropical gyres are much less productive.

# Scatterometry



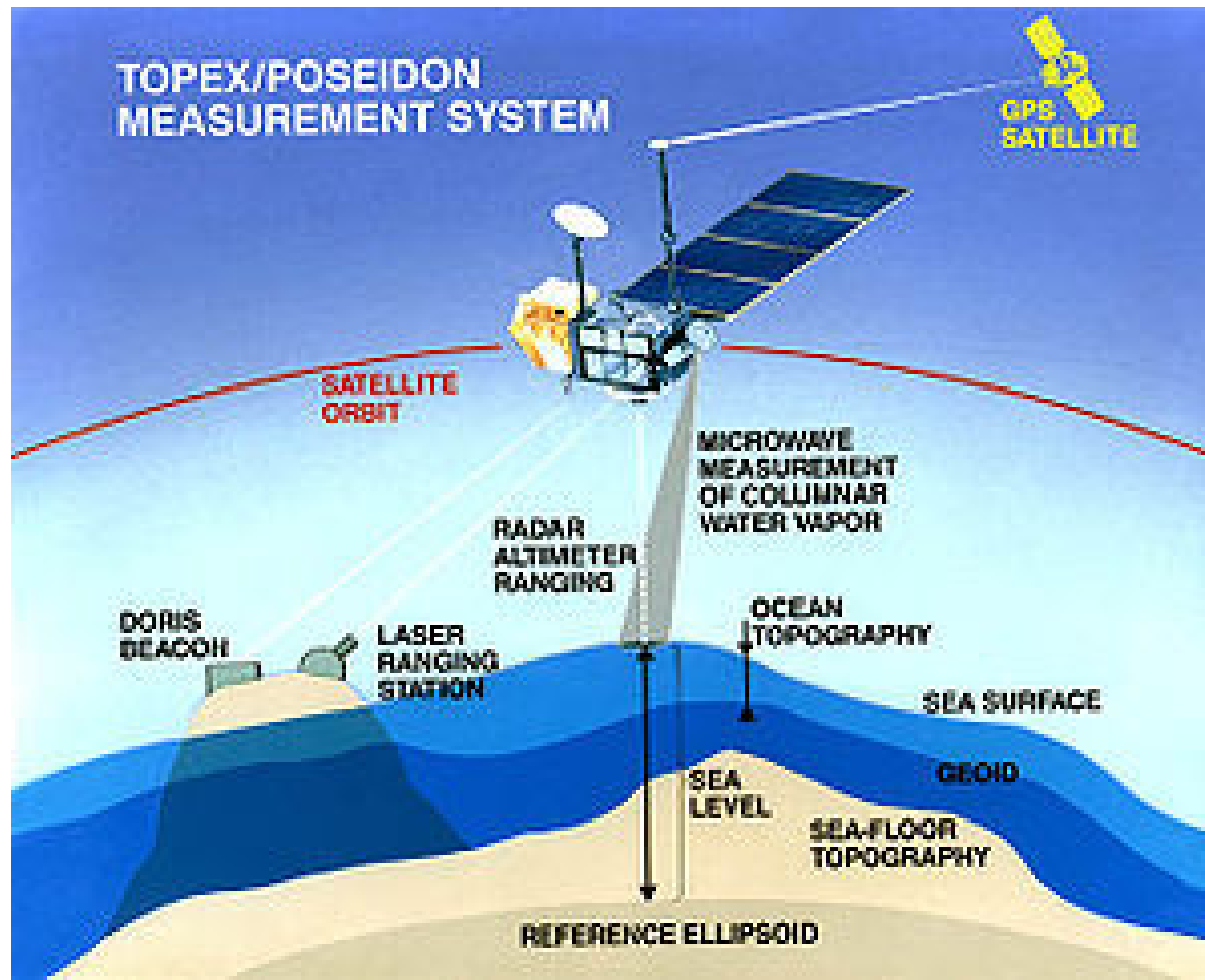
Sketch of a light wave scattering of a rough surface in an oblique-viewing microwave scatterometer. For a smooth surface oblique viewing with an active radar yields virtually no return signal. If the surface is rough, significant backscatter occurs. The roughness of the ocean surface is controlled by the shorter surface gravity waves that are generated by the local surface wind stress.

# Scatterometry: Surface Winds



Mean wind stress: (top) zonal, with eastward wind stress on the ocean positive; (bottom) meridional, with northward stress positive. Colored at  $0.02 \text{ N m}^{-2}$  intervals, with  $0.05 \text{ N m}^{-2}$  contour intervals. The dominant signals are mid-latitude westerlies and tropical trade winds, which provide forcing for gyres, equatorial currents, and the Antarctic Circumpolar Current (ACC). (Large and Yeager, 2009)

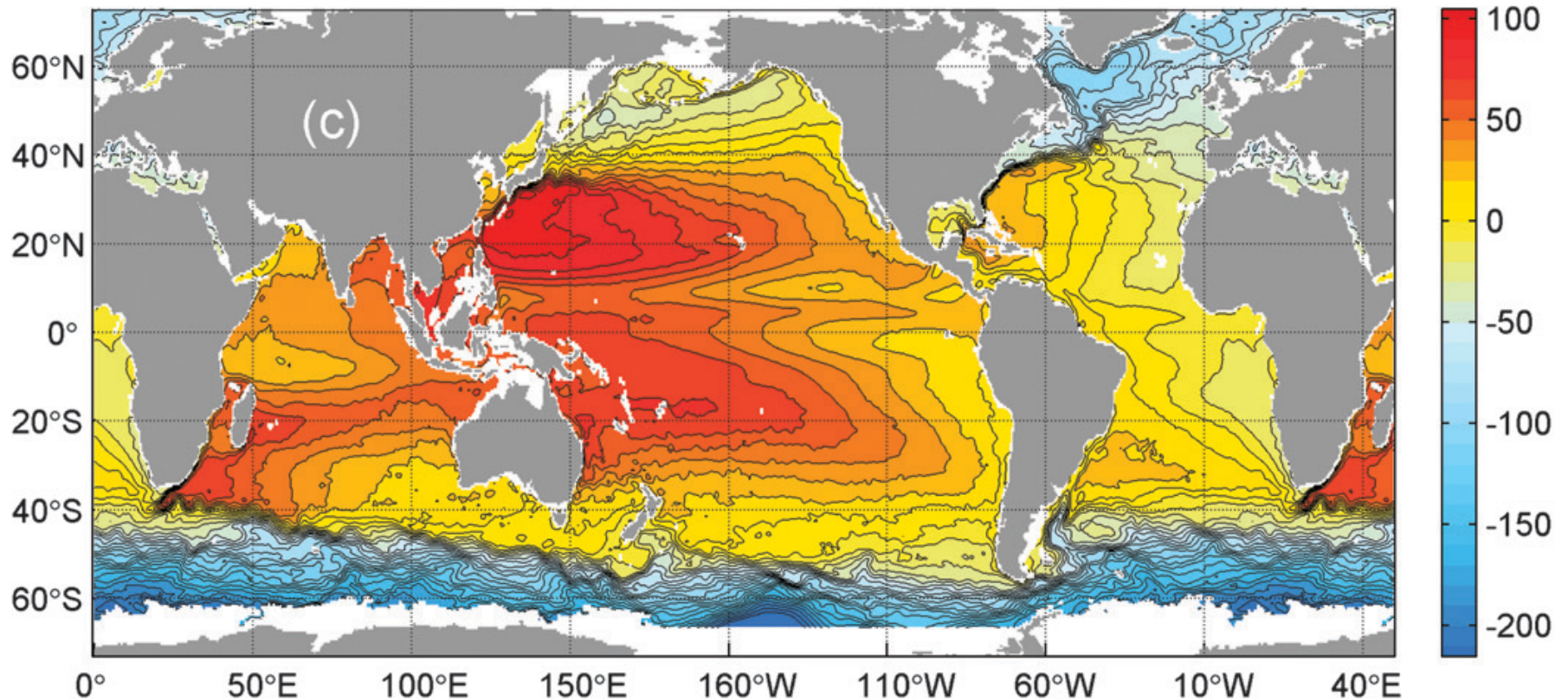
# Altimetry



A radar altimeter illuminates the oceanic surface with microwave pulses and measures the amplitude, phase, and the travel time of the reflected signal to determine the distance traveled. After determining the satellite position and correcting for the complex shape of Earth's gravitational field, this distance yields the sea surface height (SSH or  $\eta$ ) whose horizontal gradient is a pressure force, usually analyzed as part of geostrophic balance,  $f\hat{z} \times \mathbf{u}_g = -g\nabla\eta$ . SSH also includes "steric height" due to changes in vertically integrated heat content, as well as total sea mass, which changes with ice and water fluxes.



# Mean Dynamic Sea Level



Global mean sea-level  $\eta$  relative to an iso-surface of Earth's gravitational potential (*i.e.*, dynamic height) [in m with contour interval 0.1 m]. Geostrophic flow is along isolines of  $\eta$ . The mid-latitude gyres and ACC are evident. Notice that the gyres have narrow strong western boundary currents (WBC). This is an analysis from altimetry and surface drifters for the period 1993-2002.

(Maximenko *et al.*, 2009)



**Concept:** Earth's gravity field is very bumpy ( $\Delta h \sim 10\text{s m}$  near the surface) due to inhomogeneities in the solid core and mantle.

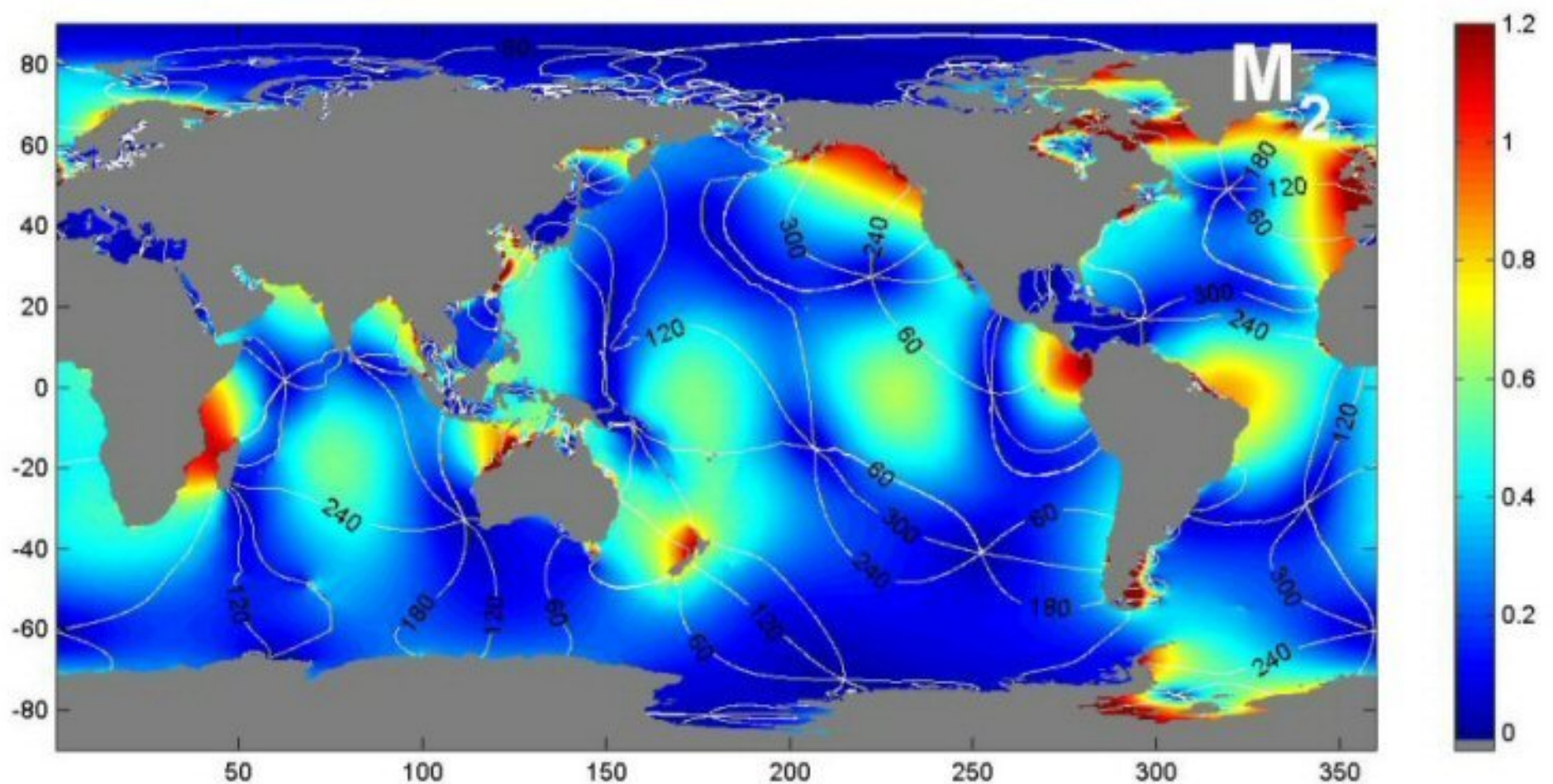
A dynamical view of sea level differences ( $\Delta h \sim 10\text{s cm}$ ) has to calculate horizontal pressure gradients relative to these bumpy gravitational equipotential surfaces.

Most large-scale surface currents  $\mathbf{u}$  satisfy a simple horizontal force balance called geostrophy:

$$f(\varphi)\hat{\mathbf{z}} \times \mathbf{u} \approx -g\nabla\eta.$$

where  $f$  the Coriolis frequency of Earth's rotation,  $\varphi$  is latitude,  $\hat{\mathbf{z}}$  is upward, and  $g$  is Earth's gravitational acceleration.

# Altimetry: Tides



Barotropic Tides: global sea-level amplitude [m] (peak-to-node) and phase [degrees in a cycle] of the M2 (lunar semi-diurnal) tide determined from satellite altimetry (Egbert and Erofeeva, 2002).

Barotropic refers to depth-averaged currents; this is the part of the tide forced directly by astronomical bodies. Flow past topography in stratified water also generates a baroclinic tide (*i.e.*, non-barotropic). Notice how spatially variable the tidal amplitude is. In small, enclosed bays and channels (not evident here), the tidal range is many meters.

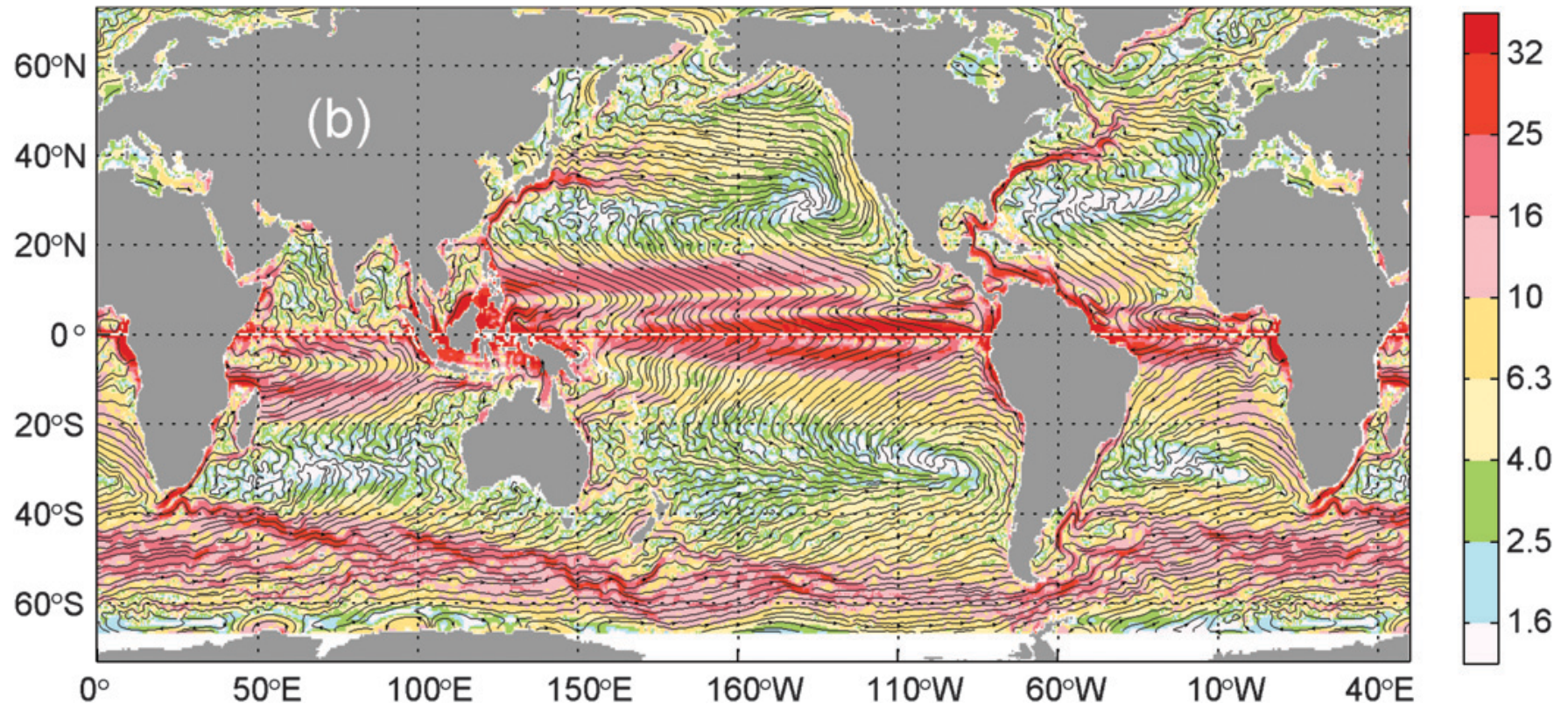
**Concept:** Tidal currents are due to the gravitational attraction of the moving sun, moon, and planets relative to the water mass at a given location on Earth.

Because “planetary” orbits are usually time-periodic, so is the gravitational forcing and primary oceanic response. (Periodicity is the exception for oceanic currents.)

An orbital period often provides a forcing at half the period; *e.g.*, when the moon is overhead (water closer than solid earth) and when it is antipodal (solid earth closer than water).

Tidal response is highly inhomogeneous, mainly due to bathymetry: strong currents in shallow, enclosed places.

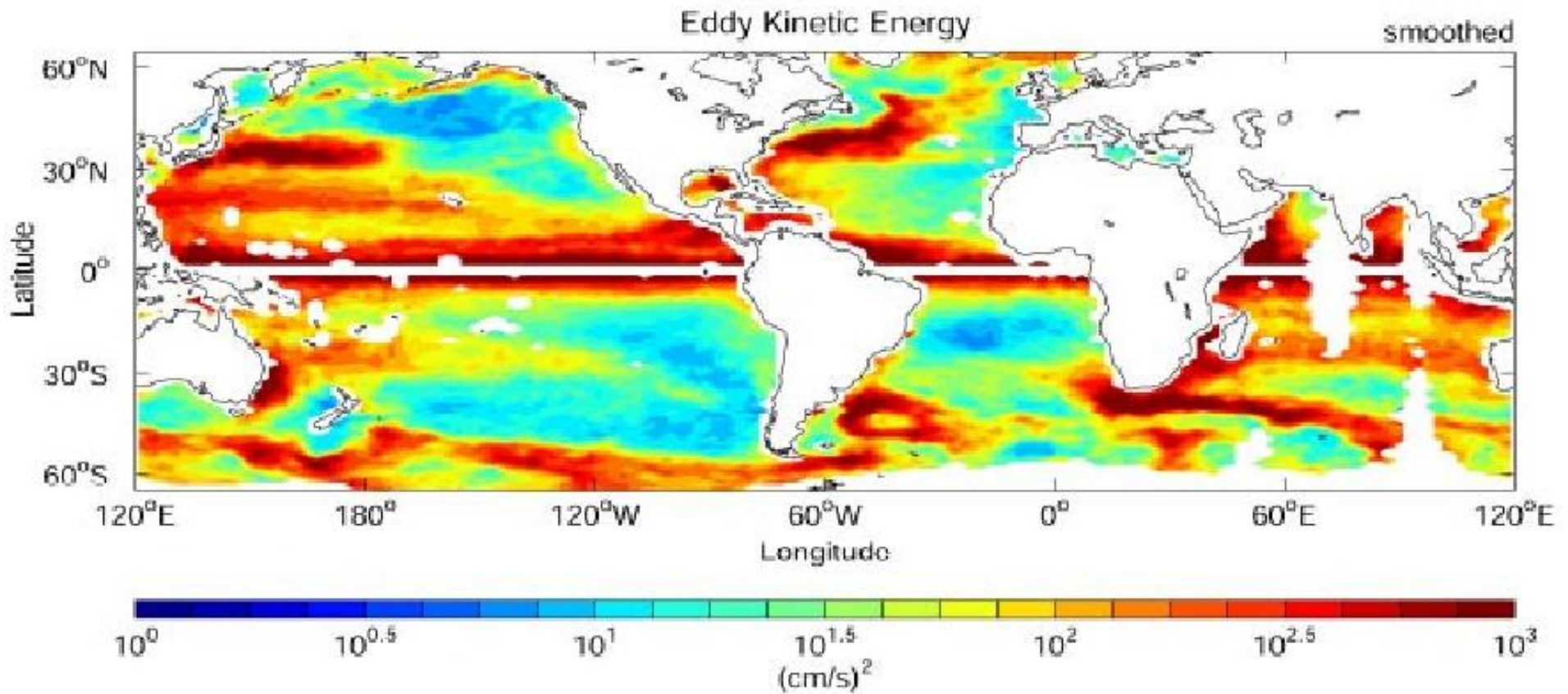
# Mean Surface Currents



Mean streamlines for surface velocity with the speed in color [ $\text{cm s}^{-1}$ ] (Maximenko *et al.*, 2009). A streamline traces the path of a particle trapped at the surface in the mean velocity field. This is an analysis from altimetry and surface drifters for the period 1993-2002. Again notice the gyres with WBCs, equatorial currents, and the ACC.



# Altimetry: Eddy Kinetic Energy

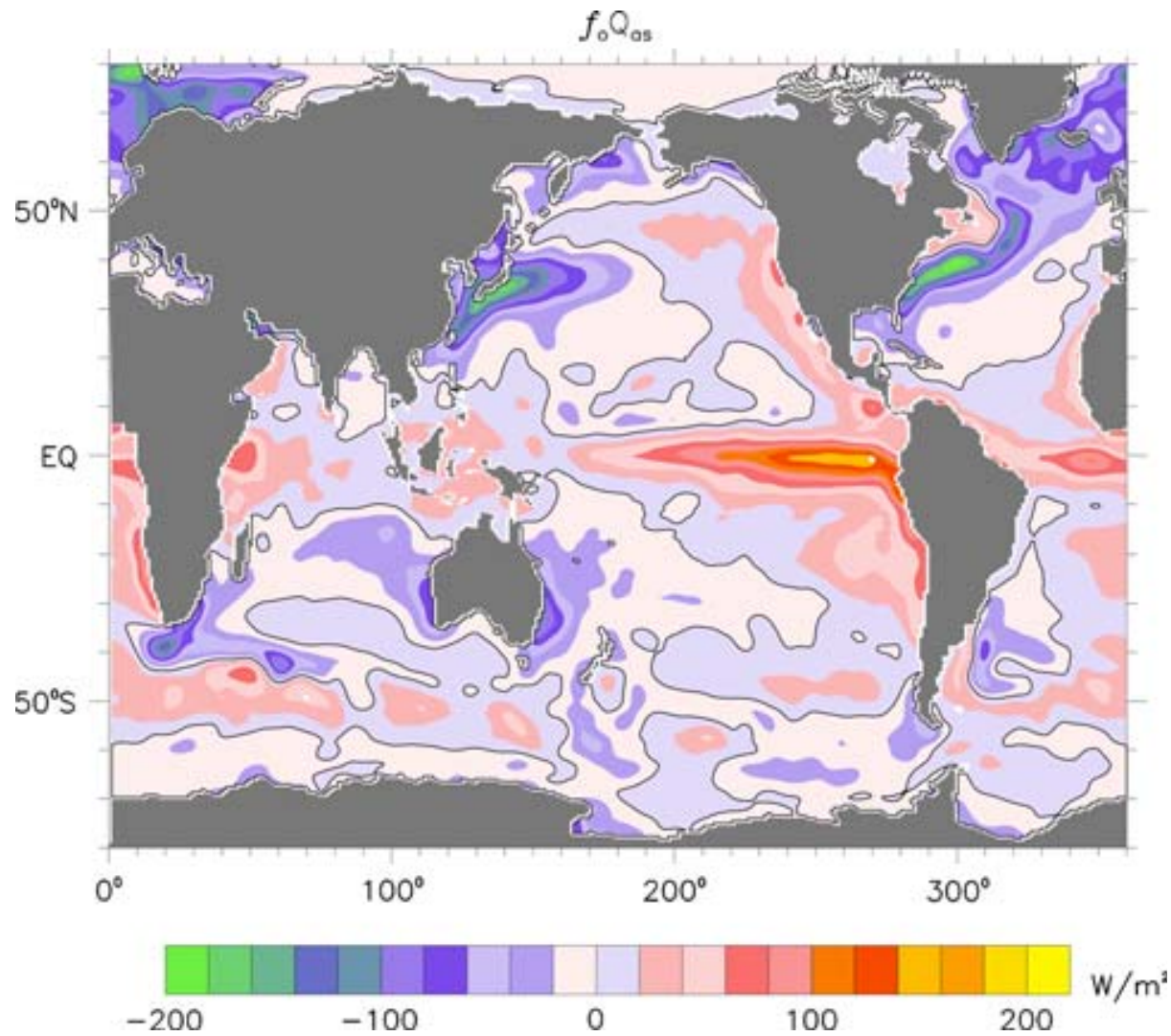


Eddy kinetic energy [ $\text{cm}^2 \text{s}^{-2}$  on a log scale] for geostrophic currents at the surface calculated from altimetric sea-level (Stammer and Scharfenberg, 2009). Eddy energy refers to time-averaged velocity variance after subtracting the mean flow. Eddies are everywhere but with highly variable strength.

They arise from instability of the mean circulation, hence are strongest in the neighborhood of strong mean currents. Mostly they are quasi-circular horizontal flows with mesoscale diameters ( $\sim 100 \text{ km}$ ) that move around and sometimes survive for many months or even years.

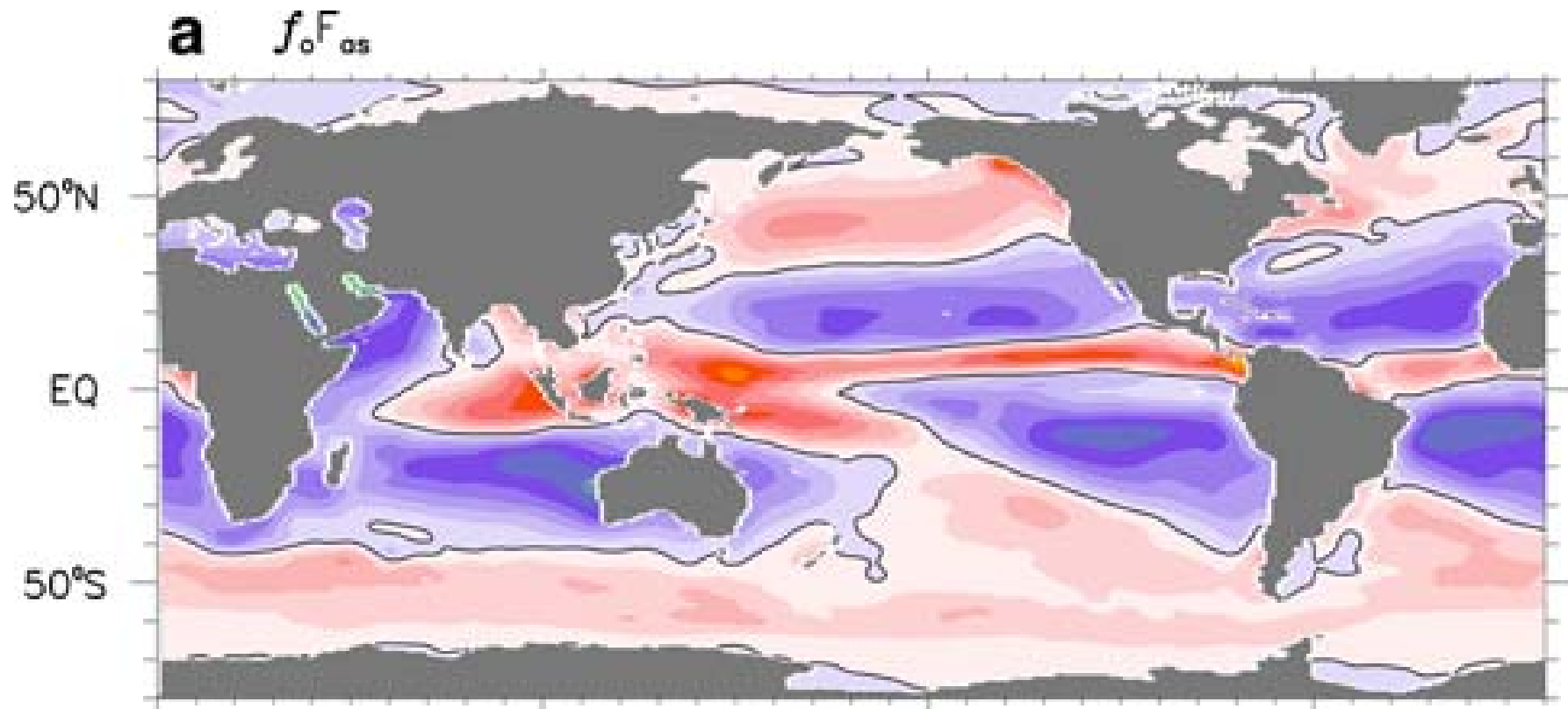


# Surface Heat Flux



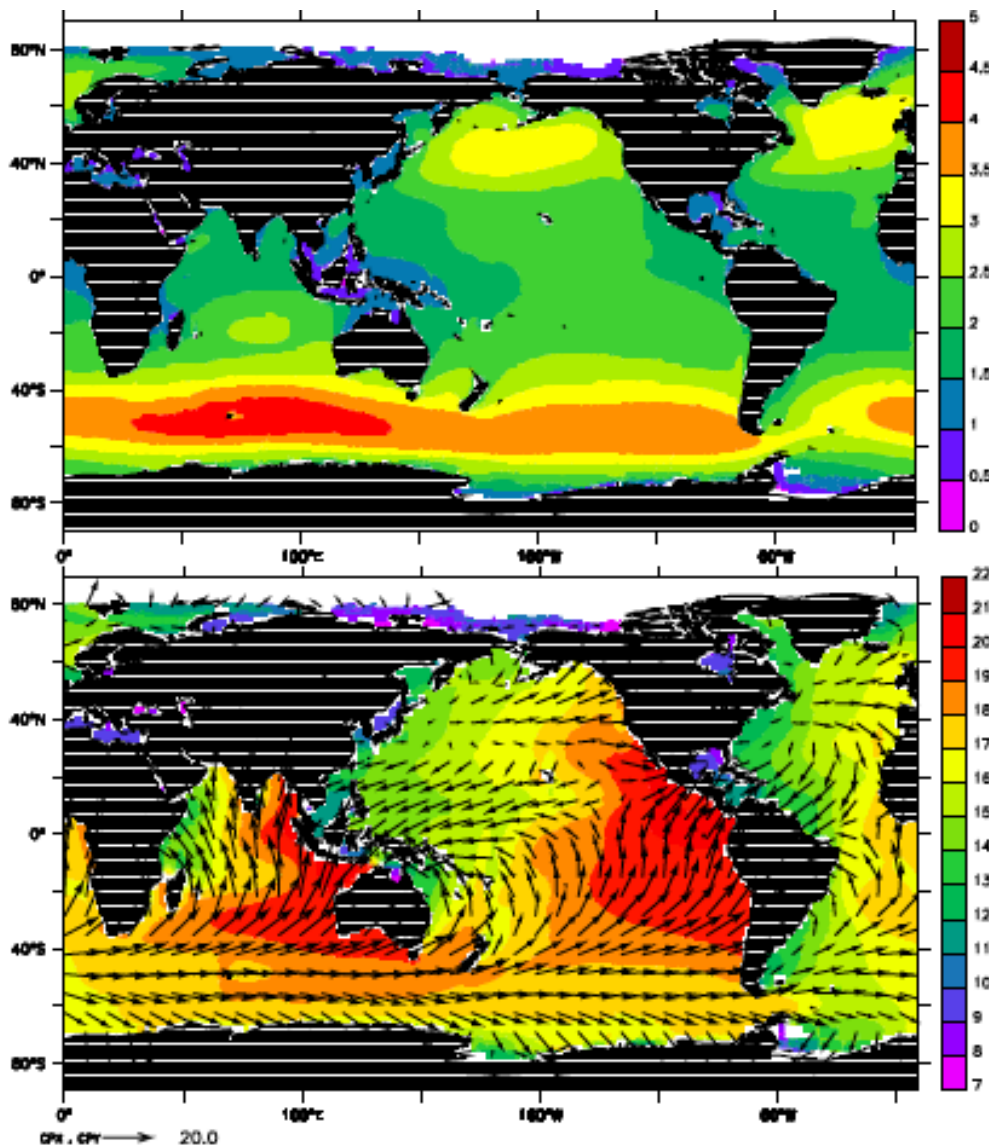
Mean surface heat flux, positive into the ocean. Colored at  $20 W m^{-2}$  intervals. This analysis comes from multiple data sources (Large and Yeagar, 2009). Broadly there is tropical heating and polar cooling, but circulation also has a strong imprint. Surface heat flux is the means by which the ocean most affects climate, and it plus surface water flux are the drivers of the global thermohaline circulation.

# Surface Fresh Water Flux



Mean surface water flux  $F$ , positive into the ocean, and colored at  $10 \text{ mg m}^{-2} \text{ s}^{-1}$  intervals. This analysis comes from multiple data sources (Large and Yeagar, 2009).  $F = \text{precipitation} + \text{run-off} + \text{sea ice melting} - \text{ice freezing} - \text{evaporation}$ . Generally  $F$  increases with latitude. Notice the Inter-tropical Convergence Zone (ITCZ) and western Pacific convection zones, and mid-latitude storm tracks with  $F > 0$ , as well as subtropical evaporation zones with  $F < 0$ . Run-off is not as evident in  $F$  here as its effect is in surface  $S$  (slide 7).

# Surface Gravity Waves



Climatology of surface gravity waves: (top) significant wave height  $H_s = 4 \text{ rms}[\eta]$  [m], and (bottom) peak phase speed and direction in  $\text{m s}^{-1}$  associated with the mean spectrum peak (Hanley *et al.*, 2010). All quantities are calculated with a wave model using the ERA-40 climate reanalysis wind data averaged over 1958 - 2001. Colors show magnitude and vectors show magnitude and direction. The biggest waves are in the storm tracks, especially near the ACC. The day to day variability of waves is high in association with storms. Swell waves can travel long distances with little decay.

**Concept:** Surface gravity waves are generated by the drag of wind over water, through an oscillatory instability of the “free surface” air-water interface.

Waves spin up rapidly when the wind increases (“wind waves”), but die away more slowly when the wind abates.

Waves can travel long distance in their slow decay phase in the form of long-period “swell” (10s of seconds). Southern California’s best surf comes from winter storms in either the subpolar North Pacific or the Pacific Antarctic.

## References

de Boyer Montegut, C., G. Madec, A. S. Fischer, A. Lazar, and D. Iudicone, 2004: Mixed layer depth over the global ocean: an examination of profile data and a profile-based climatology. *J. Geophys. Res.* **109**, C12003, doi:10.1029/2004JC002378.

Egbert, G., and S. Erofeeva, 2002: Efficient inverse modeling of barotropic ocean tides, *J. Atmos. Ocean. Tech.* **19**, 183-204.

<http://www.oce.orst.edu/research/po/research/tide/global.html>

Garcia, H. E., R. Locarnini, T. Boyer, , and J. Antonov, 2006: *World Ocean Atlas 2005* Vol. 4, Nutrients (Phosphate, Nitrate, Silicate). NOAA Atlas NESDIS 64, US Government Printing Office.

Hanley, K., S. Belcher, and P. Sullivan, 2010: A global climatology of wind-wave interaction. *J. Phys. Ocean.* In press.

Large, W. and S. Yeager, 2009: The global climatology of an interannually varying air-sea flux data set. *Climate Dyn.* **33**, 341-364.

Maximenko. N. *et al.*, 2009: Mean dynamic topography of the ocean derived from satellite and drifting buoy data using three different techniques. *J. Ocean. Atmos. Tech.* **26**, 1910-1919.

Ralph, E.A., and P.P. Niiler, 1999: Wind-driven currents in the tropical Pacific. *J. Phys. Ocean.* **29**, 2121-2129.

Les guides du SHOM, La Mare, 1997, Ref. OG941.



Stammer, D., and M. Scharfenberg, 2009: Velocity statistics interred from the TOPEX/Poseidon-JASON tandem mission. In preparation.

Stewart, Robert, 2008: *Introduction to Physical Oceanography*.

[http://oceanworld.tamu.edu/resources/ocng\\_textbook/PDF\\_files/book\\_pdf\\_files.html](http://oceanworld.tamu.edu/resources/ocng_textbook/PDF_files/book_pdf_files.html)

Weller, R., and D. Halpern, 1983: The velocity structure of the upper ocean in the presence of surface forcing and mesoscale oceanic eddies. *Phil. Trans. Roy. Soc. London* **308**, 327-340.

Whitney, F., H. Freeland, and M. Robert, 2007: Persistently declining oxygen levels in the interior waters of the eastern subarctic Pacific, *Progress in Oceanography* **75**, 179-199.

Zachos, J., M. Pagani, L. Sloan, E. Thomas, and K. Billups, 2001: Trends, rhythms, and aberrations in global climate 65 Ma to present. *Science* **292**, 686-693.